CHEMISTRY
A EUROPEAN JOURNAL

DOI: 10.1002/chem.200700413

Extended Dötz-Like Cyclization Reactions Towards the Synthesis of Eight-Membered Ring-Containing Polycycles: Scope and Theoretical Studies**

José Barluenga,* Martín Fañanás-Mastral, M. Angel Palomero, Fernando Aznar, and Carlos Valdés[a]

Abstract: The reaction between cyclobutene-containing dienyl Fischer carbene complexes (FCCs) and alkynes has been studied from both an experimental and a theoretical point of view. We have found that the reaction follows different pathways depending on the nature of the terminal double bond of the carbene complex. Thus, eight-membered carbocycles have been obtained from an extended Dötz-like reaction of dienyl FCCs and indolyl- or benzofuryl-substituted alkenyl FCCs. On the other hand, phenyl- and naphthyl-substituted alkenyl FCCs follow a typical benzannulation pathway giving rise to cyclohexadienones. DFT calculations have allowed us to formulate detailed mechanistic proposals and to provide an explanation for the formation of either the benzannulation products or the eight-membered carbocycles.

Keywords: alkynes · carbenes · density functional calculations · Fischer carbene complexes · indoles · polycycles · reaction mechanisms

Introduction

Fischer carbene complexes (FCCs) have become very useful materials in organic synthesis. During the last two decades, their chemistry has been extensively studied and at present there are a large number of useful transformations involving FCCs that find application in synthetic organic chemistry, mostly oriented towards the preparation of carbo- and heterocycles. In fact, a particularly interesting feature of the chemistry of FCCs is their ability to provide complex carbocyclic structures from simple starting materials in processes that usually involve the formation of several C–C bonds in a cascade of elementary reactions.[2]

Among the most studied processes are the reactions between FCCs and alkynes.[3] In the first instance, these reactions usually give rise to α,β-unsaturated carbene complexes derived from the insertion of the alkyne which are generally more reactive than the initial carbene and therefore evolve to form different types of products. The evolution reactions depend on the nature of the alkyne and the carbene complex and may involve insertion of another alkyne,[4] insertion of a CO ligand,[5] cyclopropanation of alkenes,[6] metallatriene cyclization,[7] α-hydrogen activation,[8] or dimerization of the carbene ligand.[9]

The well-known Dötz benzannulation reaction[10] can be regarded as the most important and synthetically useful of these reactions. In the Dötz benzannulation reaction, an alkenyl FCC and an alkyne provide a *p*-alkoxyphenol derivative. The mechanism of this reaction has been thoroughly studied both experimentally and computationally. The most accepted route is shown in Scheme 1. The first step consists of the loss of a CO ligand to generate the coordinatively unsaturated tetracarbonyl complex **I**. Then, coordination of the alkyne to the metal center leads to the η^2-alkyne(tetracarbonyl)carbene complex **II**. Insertion of the alkyne produces carbene complex **III**, which evolves by insertion of one CO ligand to yield the α,β,γ,δ-unsaturated metal–ketene complex **IV**. Finally, electrocyclic ring closure followed by tautomerization gives rise to the tricarbonylchromium-complexed alkoxyphenol **VI** and eventually to the metal-free alkoxyphenol **VII** upon decoordination.

Although the benzannulation product is commonly obtained, in some cases, upon alkyne insertion, complexes **III** can follow alternative pathways. In fact, the reaction between alkynes and α,β-unsaturated Fischer carbene com-

[a] Prof. Dr. J. Barluenga, M. Fañanás-Mastral, Dr. M. A. Palomero, Dr. F. Aznar, Dr. C. Valdés
Instituto de Química Organometálica "Enrique Moles"
Unidad Asociada al C.S.I.C., Universidad de Oviedo
Julián Clavería 8, 33006 Oviedo (Spain)
Fax: (+34) 985-103-450
E-mail: barluenga@uniovi.es

[**] Part of this work has previously been published as a communication, see ref. [1].

Supporting information for this article is available on the WWW under http://www.chemeurj.org/ or from the author.

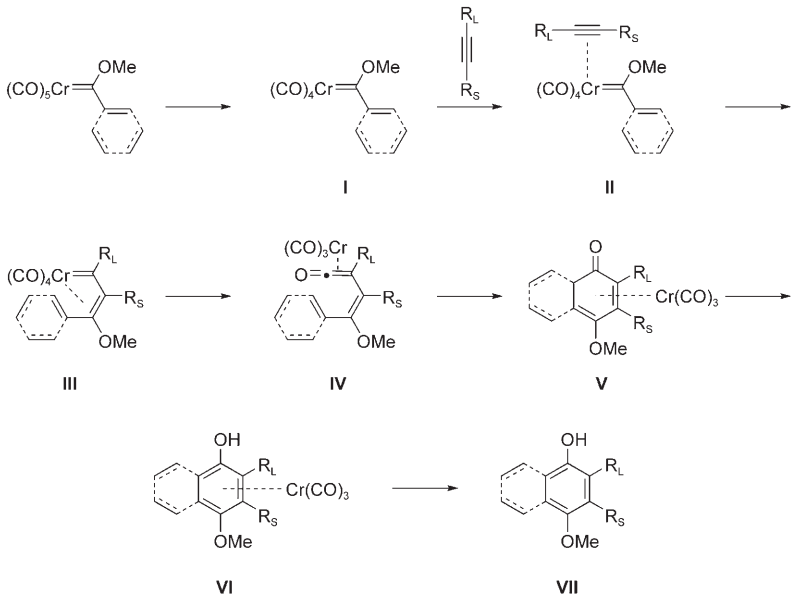

Scheme 1. Accepted mechanism for the Dötz benzannulation reaction.

plexes can produce more than 15 different types of organic compounds.[11] For these reasons, every elementary step of the Dötz reaction and its variations has been the subject of detailed experimental and theoretical studies aimed at explaining the different reaction pathways that lead to the most important by-products.[12–16]

Aside from its mechanistic appeal, the Dötz reaction holds doubtless synthetic interest as it is a regioselective method of synthesis of highly substituted phenols. In fact, the Dötz benzannulation reaction has found wide application in the synthesis of benzo[*b*]heterocycles,[17] and also as part of the synthesis of a number of natural products and biologically active substances.[18]

In recent years, we have been interested in the preparation and synthetic applications of 1-metallahexa-1,3,5-trienes.[19] These types of compounds can be regarded as analogues of the intermediate **III** of the typical Dötz benzannulation reaction. In fact, most 1-metallahexa-1,3,5-trienes are unstable and evolve through cyclopent- or benzannulation reactions. However, when the C3=C4 double bond belongs to a four-membered ring, the geometrical constraints imposed by the cyclobutene places the carbene moiety far apart from the reacting double bond, making the benzannulation reaction more difficult. Indeed, the metallatrienes **A** are stable at room temperature and evolve to the Dötz-like benzannulation products **B** only upon heating (Scheme 2).

Interestingly, we have recently reported that the same cyclobutene-containing dienyl carbene complexes **A** in the presence of alkynes give rise to cyclooctatrienones **C** in a process that could be envisioned as an extended Dötz cyclization.[1] Note, this reaction represents a new methodology for the preparation of functionalized eight-membered carbocycles. Motivated by the originality of this process and its potential synthetic interest, we decided to undertake a more detailed study of the scope of this reaction. Accordingly, we have investigated the behavior of different dienyl Fischer carbene complexes **A**, differing in the nature of the terminal double bonds which form a part of different olefinic and aromatic systems, in the presence of alkynes. In fact, we have observed that depending on the nature of the trienylcarbene, six- or eight-membered carbocycles can be obtained. Moreover, to gain a deeper understanding of the mechanisms of the different reactions, we have also performed DFT computations to explain the behavior observed for the different metallahexatrienes. Herein we present the results of our study.

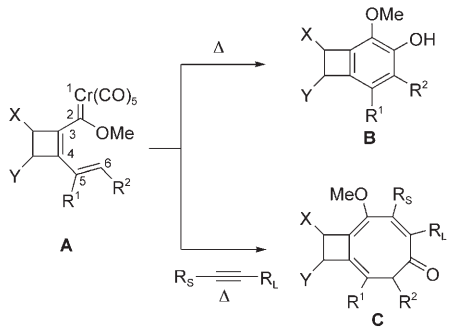

Scheme 2. Different reaction pathways of metallatrienes **A**.

Results and Discussion

Our first approach in the study of the reactions between alkynes and cyclobutene-containing metallatrienes was made using carbene complexes **2** which feature a regular double bond between C5 and C6. These types of dienyl complexes **2** are easily prepared from [2+2] cycloaddition of alkynyl carbene complexes **1** and electron-rich olefins such as enol ethers (Scheme 3).[19a]

When these dienyl carbene complexes **2** were treated with 3 equiv of a terminal alkyne in THF and warmed to reflux,

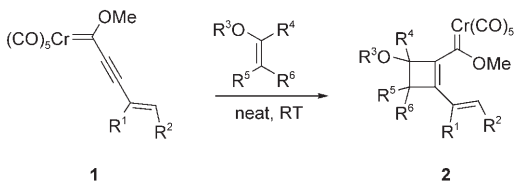

Scheme 3. Preparation of dienyl carbene complexes **2**.

the corresponding cyclooctatrienones **3** were obtained in moderate yields (Scheme 4).

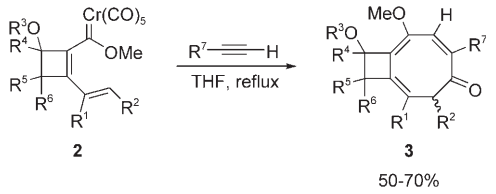

Scheme 4. Synthesis of cyclooctatrienones **3** by a Dötz-like reaction.

The reactions proceed in a regioselective fashion giving rise exclusively to the regioisomer that features the hydrogen atom of the terminal alkyne in the position closest to the methoxy group (Table 1). Compounds **3** were obtained as a mixture of diastereoisomers as a result of the newly created stereogenic center. The structure of these compounds was elucidated on the basis of their COSY and HMBC NMR spectra.

As shown in Table 1, the reaction can be conducted with a variety of dienyl carbenes and terminal alkynes, giving rise to a set of structurally diverse cyclooctatrienones. The same reaction was also carried out with internal alkynes. Symmetric systems such as tolane and bis(trimethylsilyl)acetylene were selected to avoid problems of regioselectivity. The reactions took place providing the corresponding cyclooctatrienones although with longer reaction times and lower yields. Note, although the reaction between tolane and dienyl carbene complex **2b** gave rise to the expected product **3o** (Table 1, entry 15), when bis(trimethylsilyl)acetylene was used, the loss of one TMS group occurred to give **3f** (Table 1, entry 16), the product expected from the reaction using trimethylsilylacetylene.

This process can be viewed as an extension of the Dötz reaction, as, just like in the benzannulation reaction, carbocycle formation occurs upon insertion of an alkyne and a CO molecule. However, in this case, the additional double bond present in the starting complex participates in the electrocyclic ring closure, giving rise to the eight-membered carbocycles **3**.

Interestingly, the cyclooctatrienones **3** could also be prepared in a tandem one-pot process from vinyl-substituted alkynylchromium carbene complexes **1**.[20] Thus, upon refluxing complexes **1** with three equivalents of 2,3-dihydrofuran and the alkyne in THF, the desired products were also obtained, although in slightly lower yields than in the stepwise reaction. This experimental method allowed us to carry out the reaction with the unstable and non-isolable dienyl carbene complex **2h**. The final product **3l** was obtained as a dicarbonyl compound after hydrolysis of the acetal group of **3p**, which took place during the reaction work up (Scheme 5).

We next turned our attention to the behavior of Fischer carbene complexes **4** under similar reaction conditions. The obvious difference between complexes **2** and **4** is that the terminal double bond of the latter is part of a benzene ring. Not surprisingly, when complexes **4** were refluxed in THF in the presence of 1-hexyne, the corresponding cyclooctatrienones were not obtained. Instead, as shown in Scheme 6, complexes **4** reacted with the alkyne in the fashion expected for single alkenyl complexes affording the benzannulation products **5**.

A straightforward explanation for this differential reactivity can be related to the high energy cost required to break the aromaticity of the phenyl group in the course of a hypothetical 8π-electrocyclic ring closure, which favors a Dötz-like benzannulation pathway.

With these different reactivity patterns in hand, we decided to perform a more extensive investigation of this reaction by employing dienyl carbene complexes bearing different aromatic substituents.

First of all, we examined the reactivity of naphthalene-substituted dienyl carbene complex **6** with the idea that the lower energy barrier required to involve naphthalene in an 8π-electrocyclization reaction might allow the eight-membered ring carbocycle to be obtained. However, the extended Dötz-like reaction did not take place and the benzannulation product **5c** was again obtained (Scheme 7).

To study the effect of heterocyclic substituents on the reactions of dienyl carbenes we decided to introduce an indolyl substituent to the terminus of the alkenyl carbene. With this idea, we set out to investigate the reactions of carbenes **7** and **8**, bearing an indol-3-yl and an indol-2-yl substituent, respectively, to explore the different reactivities of the C2 and C3 positions of the indole ring. Aside from the mechanistic interest of this reaction, the participation of the indole ring in an extended Dötz reaction might be a synthetically relevant transformation as it would be a new way of modifying the privileged nucleus of indole, which is found in numerous natural products and medicinally important compounds.[21]

The required alkynyl carbene complexes **9** and **10** were prepared from the 1-methyl-3-indolecarbaldehyde and 1-methyl-2-indolecarbaldehyde, respectively, by employing conventional chemistry,[22] as represented in Scheme 8. Then [2+2] cycloaddition of **9** and **10** with 2,3-dihydrofuran provided the corresponding indole-substituted dienyl carbenes **7** and **8**, respectively (Scheme 8).

When dienyl carbene complex **7** was treated with terminal alkynes in THF under reflux the corresponding cyclooct[*b*]indoles **15** were obtained in moderate yields. Similarly, when complex **8** was used as the starting product, cyclooct[*b*]indoles **16** were obtained in the same way (Scheme 9). Note, in both cases, 8π electrocyclization involving the double bond of the indole occurred,[23] indicating that the different electronic properties of the 2- and 3-substituted indoles do not affect the course of the reaction.

The reactions proceeded in a regio- and diastereoselective manner leading to a single diastereoisomer (Table 2). The relative stereochemistry between the stereocenters was determined by X-ray analysis of cyclooct[*b*]indole **16d**.

This reaction represents a very straightforward approach to cyclooct[*b*]indole, an unusual structural motif that is pres-

Table 1. Preparation of eight-membered carbocycles **3** from dienyl carbene complexes **2** and alkynes.

Entry	Carbene **2**	Alkyne	Product **3**	d.r.[a]	Yield [%][b,c]
1	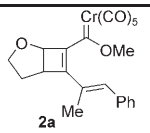 **2a**	*n*Bu—≡	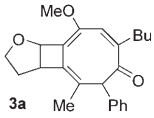 **3a**	5:1	57 (41)
2[d]	**2a**	TMS—≡	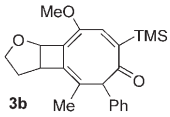 **3b**	1.4:1	63[e,f]
3	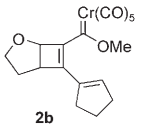 **2b**	*n*Bu—≡	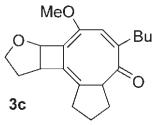 **3c**	3:1	75 (70)
4[g]	**2b**	$TBSOH_2C$—≡	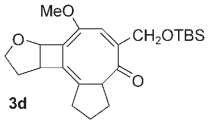 **3d**	1.3:1	59 (48)
5	**2b**	Ph—≡	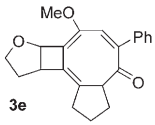 **3e**	1.2:1	61
6[d]	**2b**	TMS—≡	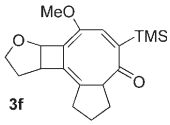 **3f**	3:1	55[e]
7[d]	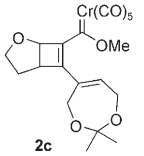 **2c**	*n*Bu—≡	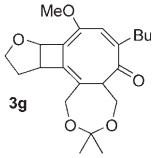 **3g**	4:1	64
8	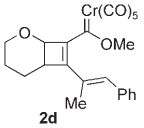 **2d**	*n*Bu—≡	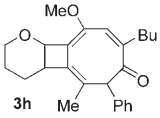 **3h**	15:1	77[h]
9	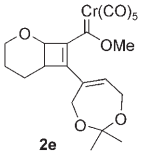 **2e**	*n*Bu—≡	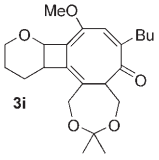 **3i**	15:1	67[h]
10	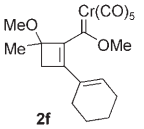 **2f**	*n*Bu—≡	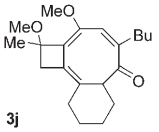 **3j**	15:1	53[h]
11	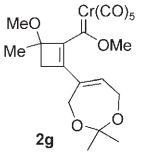 **2g**	*n*Bu—≡	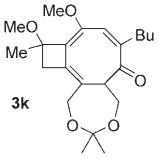 **3k**	15:1	56[h]
12	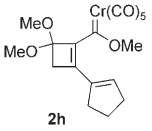 **2h**	*n*Bu—≡	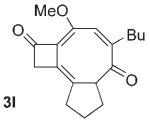 **3l**	–	52[i]

Table 1. (Continued)

Entry	Carbene **2**	Alkyne	Product **3**	d.r.[a]	Yield [%][b,c]
13	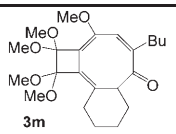 **3m**	*n*Bu—≡	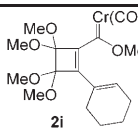 **2i**	–	52
14	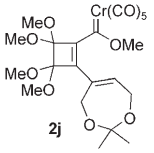 **2j**	*n*Bu—≡	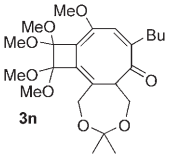 **3n**	–	60
15	**2b**	Ph—≡—Ph	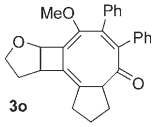 **3o**	15:1	38
16[d]	**2b**	TMS—≡—TMS	**3f**	3:1	29

[a] Determined by integration of the ^{1}H NMR signals in the crude reaction mixture. [b] Yield of isolated product based on the starting Fischer carbene complex. [c] Results in parentheses refer to the one-pot process from the corresponding alkynyl carbene complex **1**. [d] TMS = trimethylsilyl. [e] Diastereoisomers could not be separated by chromatography. [f] 20% of the product was isolated as the [$Cr(CO)_3$] complex. [g] TBS = *tert*-butyldimethylsilyl. [h] Only the major diastereoisomer was isolated. [i] Yield of the one-pot process from the corresponding alkynyl carbene complex. Ketal deprotection occurred during work up of the reaction.

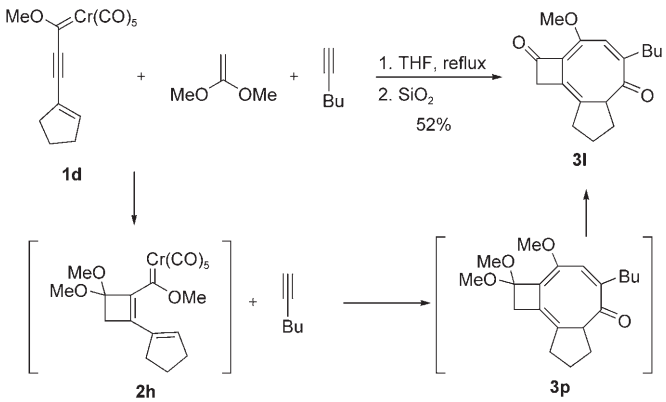

Scheme 5. Tandem one-pot process to obtain cyclooctatrienone **3l**.

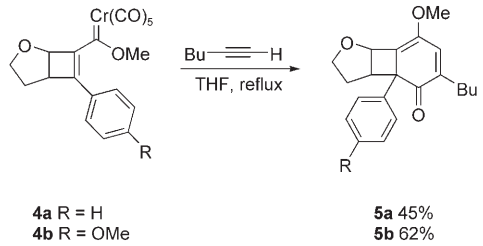

Scheme 6. The reaction between dienyl carbene complexes **4** and 1-hexyne giving rise to the benzannulation products **5**.

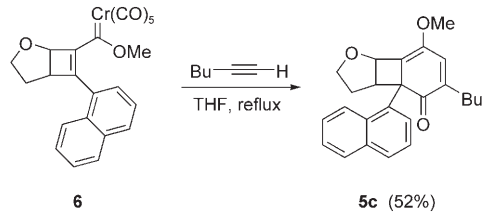

Scheme 7. Reaction between dienyl carbene **6** and 1-hexyne leading to benzannulation product **5c**.

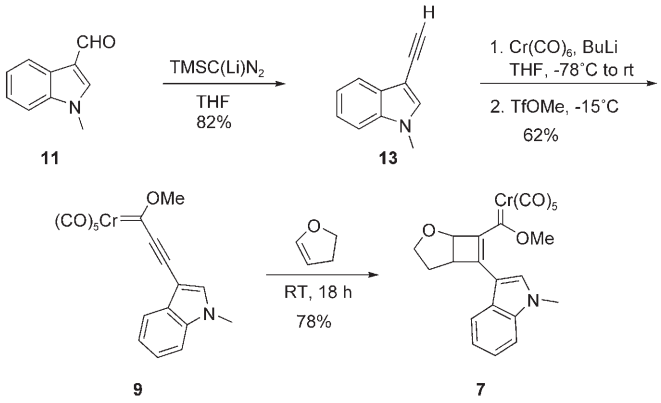

Scheme 8. Preparation of Fischer carbene complexes **9** and **7**, the identical procedure was applied for **10** and **8**.

ent in some biologically active indole alkaloids such as caulerpin[24] and dregamine isomethine.[25]

As in the preceding reactions with cyclooctatrienones **3**, polycycles **15** and **16** could be prepared in a tandem one-pot process from Fischer carbene complexes **9** and **10**, respectively, avoiding the isolation and purification of indolyl complexes **7** and **8**. In a typical example, after stirring the carbene complex **9** or **10** in THF with three equivalents of 2,3-dihydrofuran at room temperature, the corresponding alkyne was added and the mixture refluxed for 2 hours to obtain polycycles **15** and **16** in similar yields to the stepwise reaction.

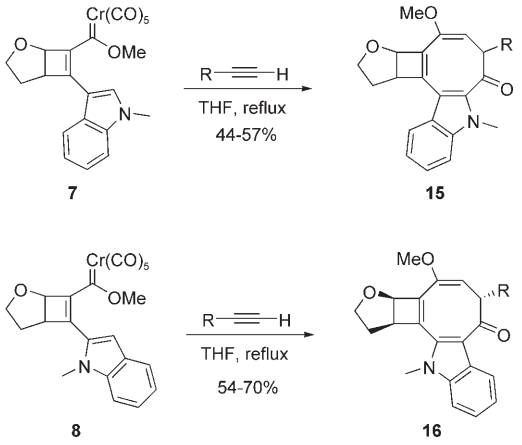

Scheme 9. Synthesis of cyclooct[*b*]indoles **15** and **16**.

Table 2. Reactions between Fischer carbene complexes **7** and **8** and terminal alkynes.

Carbene complex	R	Product	Yield [%][a,b]
7	Bu	**15a**	47 (50)
7	C_8H_{17}	**15b**	44 (49)
7	CH_2CH_2Ph	**15c**	56 (57)
8	Bu	**16a**	54 (58)
8	Ph	**16b**	57 (63)
8	CH_2Ph	**16c**	66 (68)
8	CH_2CH_2Ph	**16d**	70 (69)

[a] Yield of isolated product based on the starting Fischer carbene complex **7** and **8**. [b] Results in parentheses refer to the one-pot process from the corresponding alkynyl carbene complexes **9** and **10**.

The one-pot process was also studied with a conjugated enyne. Thus, reaction between carbene complex **10**, 2,3-dihydrofuran and 2-methylbut-1-en-3-yne led to the carbocycle **17** after isomerization of the terminal olefin (Scheme 10). Note, no side-product from a reaction between the carbene complex and the double bond of the enyne was observed.[6]

The reaction between dienyl carbene complexes **7** and **8** and terminal alkynes leading to cyclooct[*b*]indoles **15** and **16**, respectively, turned out to be quite general. However, when the substituent of the terminal alkyne is a very bulky group (R′ = TMS, *t*Bu), formation of the eight-membered ring was not observed. In these cases, the reaction gave rise exclusively to benzannulation products **18** and **19** (Scheme 11). The presence of bulky substituents probably

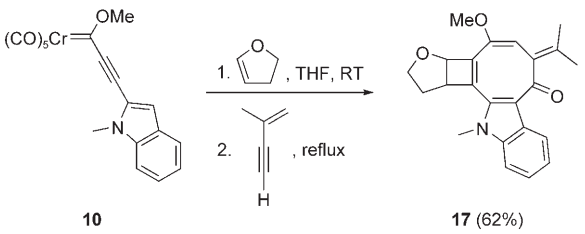

Scheme 10. Reaction between carbene complex **10** and 2-methylbut-1-en-3-yne in a tandem one-pot process.

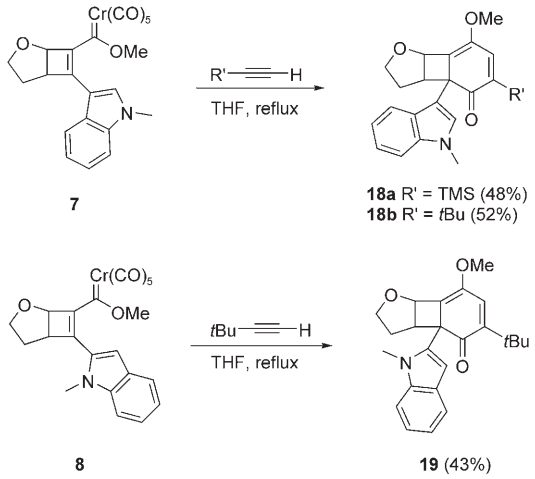

Scheme 11. Reactions of dienyl carbene complexes **7** and **8** with alkynes containing bulky groups, giving rise to benzannulation products **18** and **19**.

causes a distortion in the bond angles, favoring the formation of the six-membered ring.

The same reactivity trend observed for the indolyl complexes was also followed by the Fischer carbene complex **20** derived from a benzo[*b*]furan ring. This carbene complex, under the typical conditions of the one-pot process, gave rise to the corresponding benzo[*b*]cycloocta[*d*]furans **21** (Scheme 12). However, in this case, the eight-membered carbocycles were obtained as a mixture of diastereoisomers in relatively poor yields.

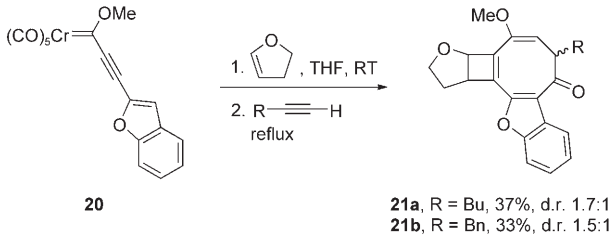

Scheme 12. Synthesis of carbocycles **21**.

Mechanistic considerations: The formation of **3**, **5**, **15**, **16** and **21** might be explained by a mechanism in which the initial steps, leading to intermediate **24**, are identical to those proposed for the Dötz reaction. As shown in Scheme 13, intermediates **22**, **23** and **24** are analogous to the intermediates proposed in the accepted mechanism of the Dötz benzannulation reaction (**II**, **III** and **IV** in Scheme 1).

The key step in the reaction between dienyl carbene complexes and alkynes is the electrocyclic ring closure of **24** and the outcome of the reaction depends on the nature of the C6=C7 double bond. When this double bond is part of an aromatic six-membered ring (phenyl or naphthyl), intermediate **24** undergoes a 6π-electron electrocyclization step leading to cyclohexadienones **5**. However, when the terminal double bond is part of an alkene or a five-membered

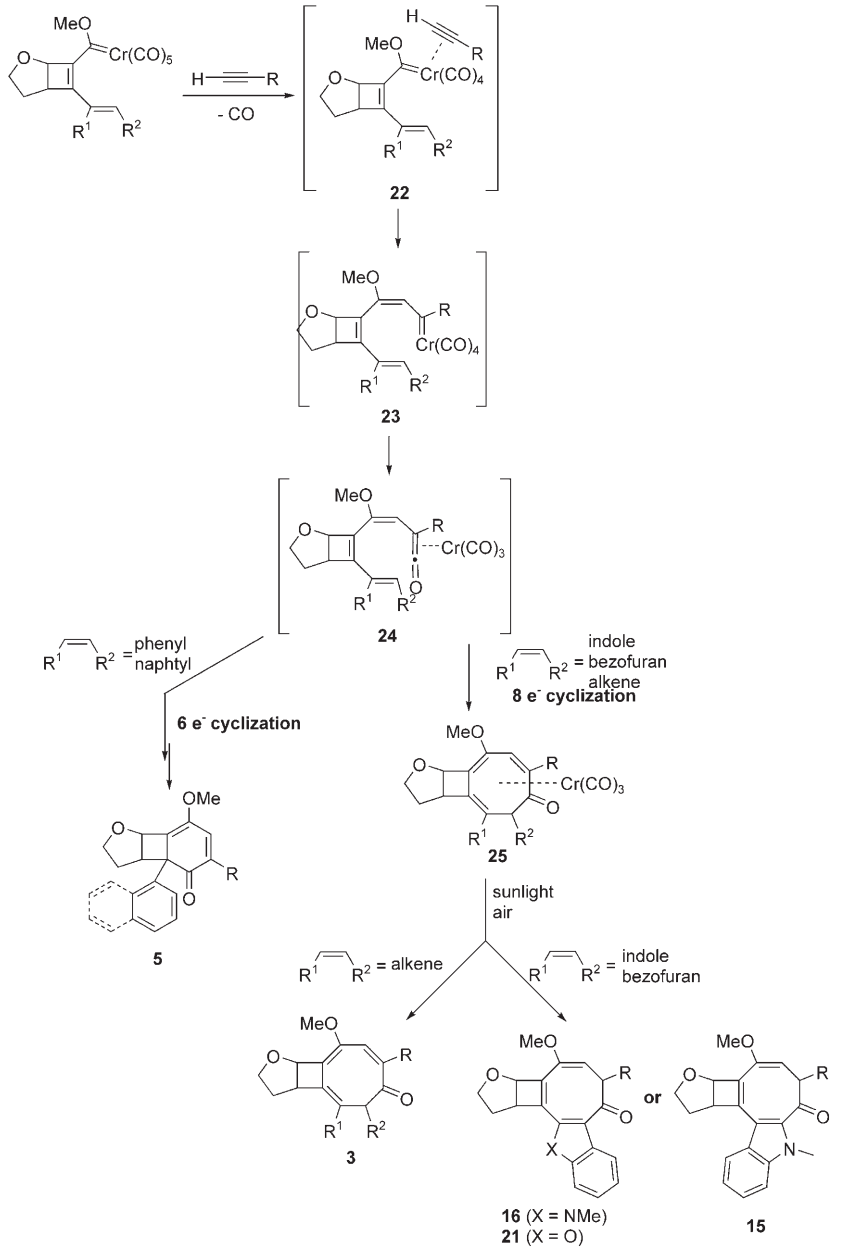

Scheme 13. Proposed mechanism for the reaction between Fischer dienyl carbene complexes and alkynes.

ring of a benzo-fused heterocycle, **24** evolves through an 8π-electron electrocyclization step, giving rise to cyclooctatrienone derivatives with the general structure **3**. In the reactions of indole and benzofuran derivatives, the final step is the aromatization of the heterocyclic group leading to cyclooct[*b*]indoles **15** and **16** or benzo[*b*]cycloocta[*d*]furans **21**.

Computational studies: To gain a deeper understanding of the different reaction pathways leading to either benzannulation or the formation of cyclooctatrienones, we carried out DFT calculations on three different model systems. We have assumed the acetylene insertion process. This initial part of the reaction mechanism is well-established as it has been extensively studied by both computational[16c,d,26] and experimental methods[12–16] for the Dötz reaction. Moreover, the acetylene insertion process is common to both the benzannulation and the formation of the eight-membered ring. Therefore, we restricted the computational study to the part of the reaction that determines the formation of the different products and performed our modelling studies starting from the intermediates with the general structure **X** (Figure 1).

We studied three model systems that cover the different chemical behavior observed experimentally. First, the trienylcarbene complex **A**, in which a pendant olefinic double bond participates in the formation of the eight-membered ring, and then two different aromatically substituted systems, the phenyl-substituted dienyl carbene **Ph**, which yields the typical benzannulation product, and the indole-substituted dienyl carbene **In**, which again provides the eight-membered ring complex.

A representation of the different reaction pathways found in our study of simple model system **A** is shown in Figure 2 and the reaction profile in Figure 3.

We found three isomeric energy minima for tetracarbonyl **A** in which the coordination vacancy of the chromium is stabilized by complexation with the vicinal double bond **A1**, the internal double bond of the cyclobutene **A2** and the pendant terminal double bond **A3** (Figure 4). Isomer **A2** is stabilized by η^2 bonding with the internal cyclobutene double bond. The presence of a complex with a structure similar to **A2** was proposed by Solà and coworkers as an intermediate in the lowest-energy reaction profile for the Dötz benzannulation reaction.[16d] Moreover, we have previously reported the characterization of a hexatriene(tetracarbonyl)chromium complex that features this particular complexation mode.[12c] In the complex **A3**, the hexatrienic moiety adopts a helical structure which allows for a nearly perfect η^2 interaction between the terminal double bond and the tetracarbonylchromium, the C–Cr dis-

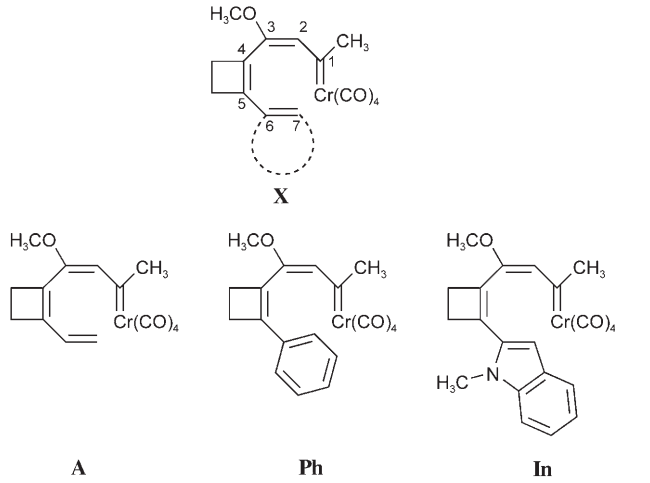

Figure 1. Model systems studied.

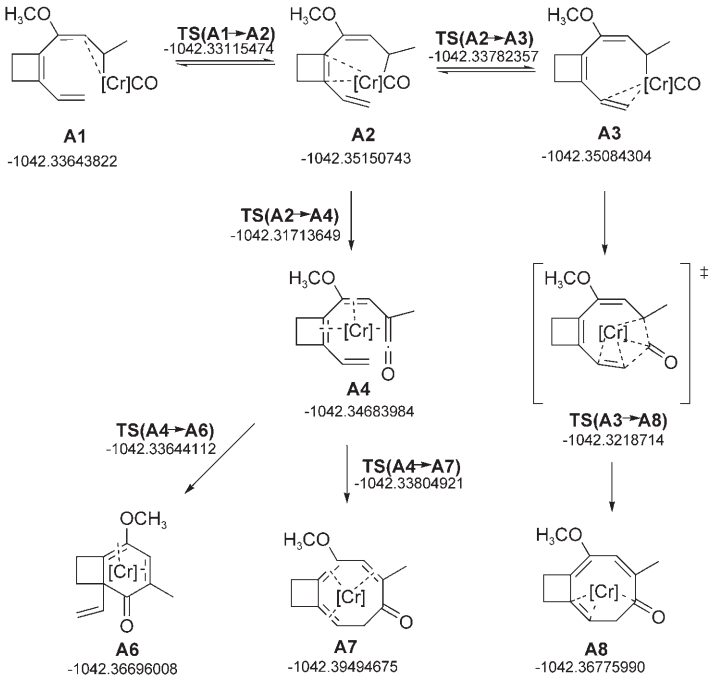

Figure 2. Calculated reaction pathways for system **A**, with the B3LYP electronic energies obtained (hartree).

tances being almost identical: d(C7–Cr) = 2.34 Å and d(C6–Cr) = 2.38 Å. Complexes **A2** and **A3** are very similar in energy. In contrast, complex **A1** is clearly less stable than **A2** (9.6 kcal mol^{-1}) as a result of the weak stabilization of the chromium coordination vacancy by the vicinal double bond. The interconversion between these three structures occurs by simple rotation of the tetracarbonylchromium moiety over the plane defined by the dienic structure. The barriers to conversion are relatively low and therefore it is expected that an equilibrium between these three structures must exist.

In analogy with the typical Dötz benzannulation reaction, the following step en route to the cyclization must be the CO insertion. Insertion of CO into complex **A2** leads to the new ketene complex **A4**, which features the $Cr(CO)_3$ moiety coordinated in a η^5 mode to the triene. At this level of theory, **A4** was found to be 4.0 kcal mol^{-1} less stable than its precursor **A2**. A high activation barrier of 22.4 kcal mol^{-1} was obtained for the conversion of **A2** to **A4** through **TS(A2→A4)**. On the other hand, after extensive calculations, we were not able to find a transition-state structure involving CO insertion starting from **A1**.[27]

Complex **A4** might evolve to generate the tricarbonylchromium-complexed cyclohexadienone **A6** (not observed experimentally) through **TS(A4→A6)** in an annulation process that resembles a six-electron disrotatory electrocyclization. An activation energy barrier of 7.8 kcal mol^{-1} was found for this transformation. On the other hand **A4** may also lead to the tricarbonylchromium-complexed cyclooctatrienone **A7** through the **TS(A4→A7)** structure in an 8π-electron conrotatory electrocyclization. The formation of the eight-membered ring has an even lower energy barrier (5.6 kcal mol^{-1}).

A different reaction pathway to another cyclooctatrienone chromium complex was also found starting from complex **A3**. We did not find a transition-state structure connecting **A3** with ketene **A4**. Instead, while searching for a TS for the carbonyl insertion, we found a different saddle point **TS(A3→A8)** which connects **A3** directly to the cyclooctatrienone complex **A8**. Intrinsic reaction coordinate (IRC) calculations confirmed that **A3** and **A8** are indeed connected through **TS(A3→A8)**. The concerted transformation from **A3** to **A8** involves the formation of two C–C bonds between the CO and both ends of the seven-membered carbon chain. Moreover, the $Cr(CO)_3$ moiety is partially stabilized by complexation through two η^2 interactions, with the double bond and with the carbonyl. The activation energy found for this process is 19.2 kcal mol^{-1}. Indeed, this is the lowest-energy reaction pathway found for the thermal rearrangement of **A1**, **A2** or **A3**. The **TS(A3→A8)** is 3.2 kcal mol^{-1} more stable than **TS(A2→A4)**, the highest energy point in the alternative reaction pathway. Thereby, our calculations are in agreement with the experimental observations and suggest the formation of the cyclooctatrienone chromium complex **A8** in an unusual single concerted step from **A3** through **TS(A3→A8)**.

The most outstanding results for the calculations on model system **Ph** are represented in Figure 5 and Figure 6. Two minimum structures **Ph1** and **Ph2** were found for the phenyl-substituted chromahexatriene. Interestingly, a structure analogous to **A3**, in which the coordination vacancy of the chromium is stabilized by the benzene ring, was not found as a stationary point on the potential energy surface. The structural characteristics found for **Ph1** and **Ph2** are very similar to those obtained for the system **A**. Also, **Ph2** is clearly more stable than **Ph1**, by an energy difference of 8.8 kcal mol^{-1}.

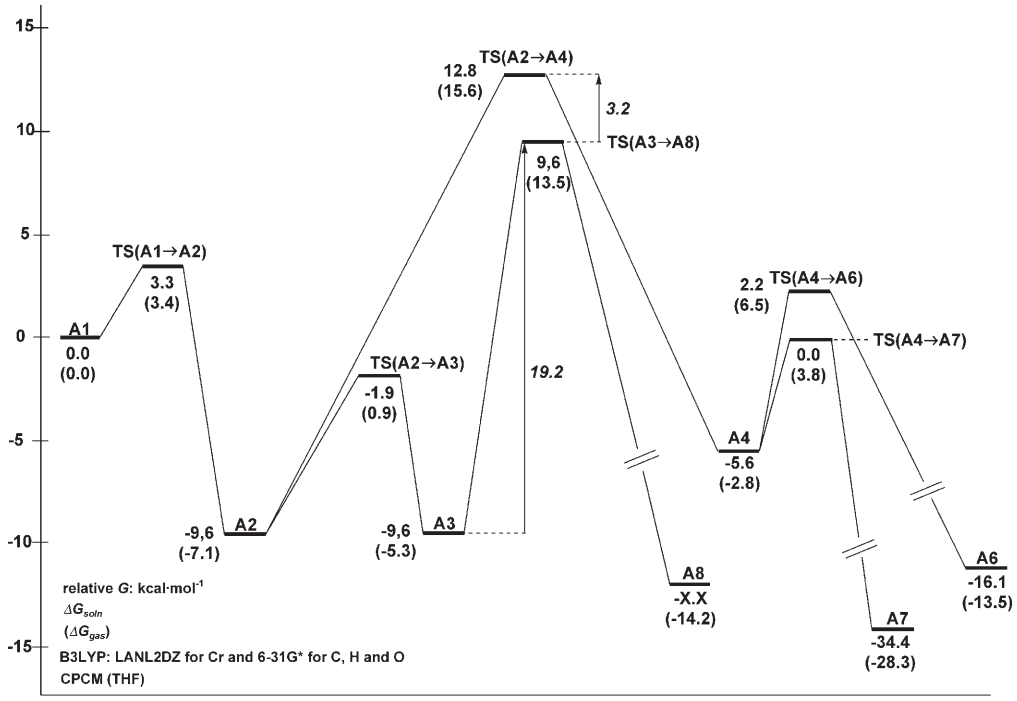

Figure 3. Gibbs energy profiles for system **A** in solution. Relative Gibbs energies in the gas phase are indicated in parentheses.

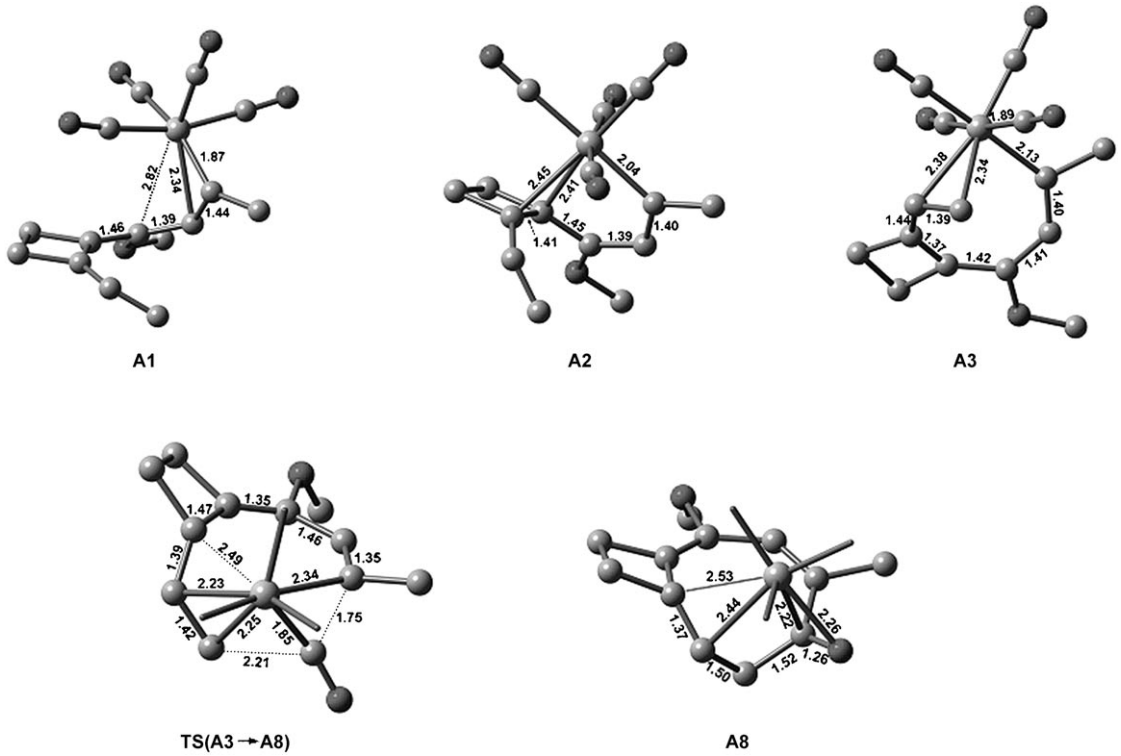

Figure 4. B3LYP-optimized structures for **A1**, **A2**, **A3**, **TS(InA3→A8)** and **A8**. Hydrogen atoms have been omitted for clarity. The CO ligands on the $Cr(CO)_3$ moiety have been removed from the models of **TS(InA3→A8)** and **A8**.

We found two alternative reaction pathways leading to the ketene complex **Ph4**. Insertion of CO into **Ph2** leads directly to the new complex **Ph4** through **TS(Ph2→Ph4)**. This transformation features a high energy barrier of 23.4 kcal mol^{-1}. Similarly to system **A**, **Ph4** was found to be 3.5 kcal mol^{-1} less stable than its precursor **Ph2**. On the

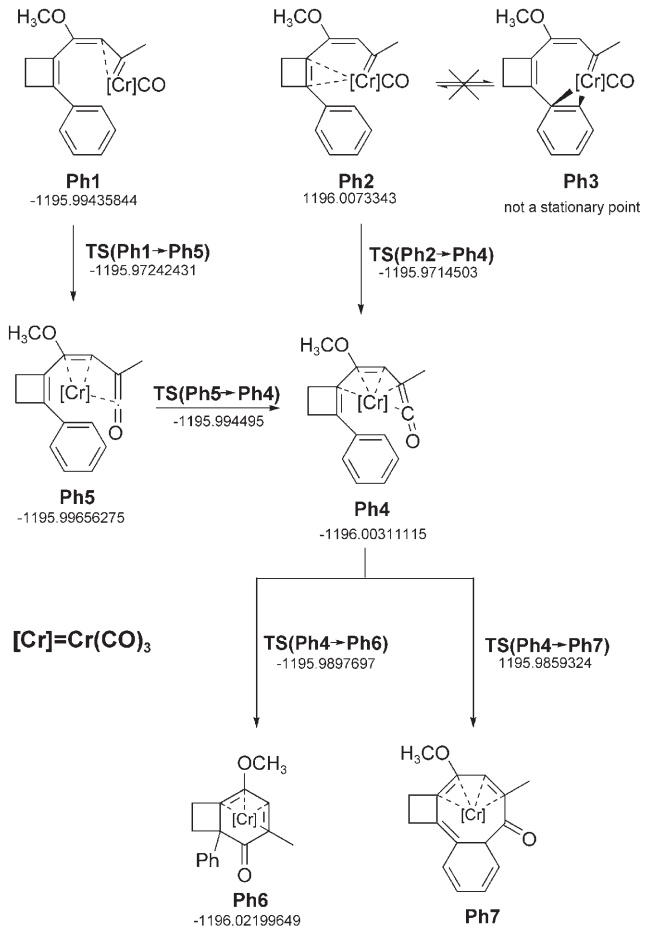

Figure 5. Reaction pathways found for system **Ph**. B3LYP electronic energies are indicated in hartrees.

other hand, CO insertion into complex **Ph1** affords the new complex **Ph5** through the **TS(Ph1→Ph5)** transition-state structure ($\Delta G_{act} = 14.3$ kcal mol^{-1}). Note that a similar TS could not be found for the **A** series. Complex **Ph5** isomerises to **Ph4** through a very low barrier (1.1 kcal mol^{-1}). This time, the **Ph1→Ph5→Ph4** pathway turned out to be the lowest energy pathway to **Ph4**, even though a very small energy difference was found between **TS(Ph2→Ph4)** and **TS(Ph1→Ph5)**. The calculated three-dimensional models for the species involved in these transformations are represented in Figure 7.

Intermediate **Ph4** can evolve to six-membered ring **Ph6** or eight-membered ring **Ph7** via **TS(Ph4→Ph6)** and **TS(Ph4→Ph7)**, respectively. The transition-state structure for the formation of the six-membered ring **TS(Ph4→Ph6)** was found to be 1.2 kcal mol^{-1} more stable than **TS(Ph4→Ph7)**, the transition state for the formation of the eight-membered ring (Figure 8). The influence of the solvent is remarkable in this case, as a much higher barrier of 3.1 kcal mol^{-1} was obtained in the gas phase. Moreover, single-point energy calculations with a larger basis set (6-311+G** for carbon, hydrogen and oxygen atoms, using the LANL2DZ ECP for chromium) provided a larger energy gap between both TSs ($\Delta E_{elec} = 3.2$ kcal mol^{-1} for the larger basis set and 2.4 kcal mol^{-1} for the standard one). Thus, the formation of **Ph6** is kinetically favoured, although by a relatively small free energy gap. On the other hand, the formation of **Ph7** is an endergonic process as a result of the disruption of the aromaticity of the phenyl ring. Therefore, even if the unstable cyclooctatrienone **Ph7** were formed, it would revert to **Ph4**. As a result, the formation of **Ph6** is also thermodynamically favoured. Taking into account the small energy difference between the transition states, both kinetic and thermodynamic effects may be responsible for the exclusive formation of **Ph6**. These results are consistent with experimental observations as **Ph6** is the only compound observed in this reaction.

The results obtained for the indolyl-substituted system **In**, represented in Figure 9, are again slightly different to those obtained for models **A** and **Ph**. This time, as in the olefin-substituted system **A**, we found three energy minima for the tetracarbonyl complex, **In1**, **In2**, and **In3**. However, the stabilization of the tetracarbonyl by donation of the double bond of the indole in **In3** is much weaker than in **A3**. As a consequence, **In2** is clearly the most stable species, while **In1** and **In3** have similar higher energies. Moreover, complex **In3** does not participate in the following steps as the transformation of **In3** into **In8** has a very high energy barrier (Figure 10).

As in the phenyl-substituted **Ph** system, carbonyl insertion to give **In4** can follow two different pathways. The optimized structures obtained for both sequences are nearly identical to those found for the **Ph** series (Figure 11). Again, both transition states are very similar in energy, **TS(In2→In4)** being 1 kcal mol^{-1} more stable than **TS(In1→In5)** taking into account the solvation energy, while the latter was found to be 1.1 kcal mol^{-1} more stable in the gas phase. Either way, the formation of the six- or eight-membered ring must proceed through the ketene **In4** and the chemoselectivity of the process will be determined by the relative energies of the corresponding transition states **TS(In4→In6)** and **TS(In4→In7)**, respectively. Interestingly, **TS(In4→In7)**, the transition state that leads to the formation of the cyclooctatrienone, was found to be 5.7 kcal mol^{-1} more stable than **TS(In4→In6)**. These results are in agreement with experimental observations, as for the indolyl-substituted systems the cyclooctatrienone is the only compound obtained.

In order to explain the different behavior of the phenyl-substituted system **Ph** compared with the indole system **In** and olefin-substituted system **A**, it is very revealing to examine the structures of the transition states that lead to the formation of either the six- or the eight-membered rings for the three series. According to our modelling studies, the transition states **TS(A4→A6)**, **TS(Ph4→Ph6)** and **TS(In4→In6)**, which lead to the six-membered ring complexes **A6**, **Ph6** and **In6**, respectively, resemble a disrotatory 6π-electron electrocyclization with the $Cr(CO)_3$ moiety as spectator on top of the plane defined by the hexatriene structure. The pericyclic nature of these annulations becomes apparent by analysing the nearly identical C–C bond distances of the in-

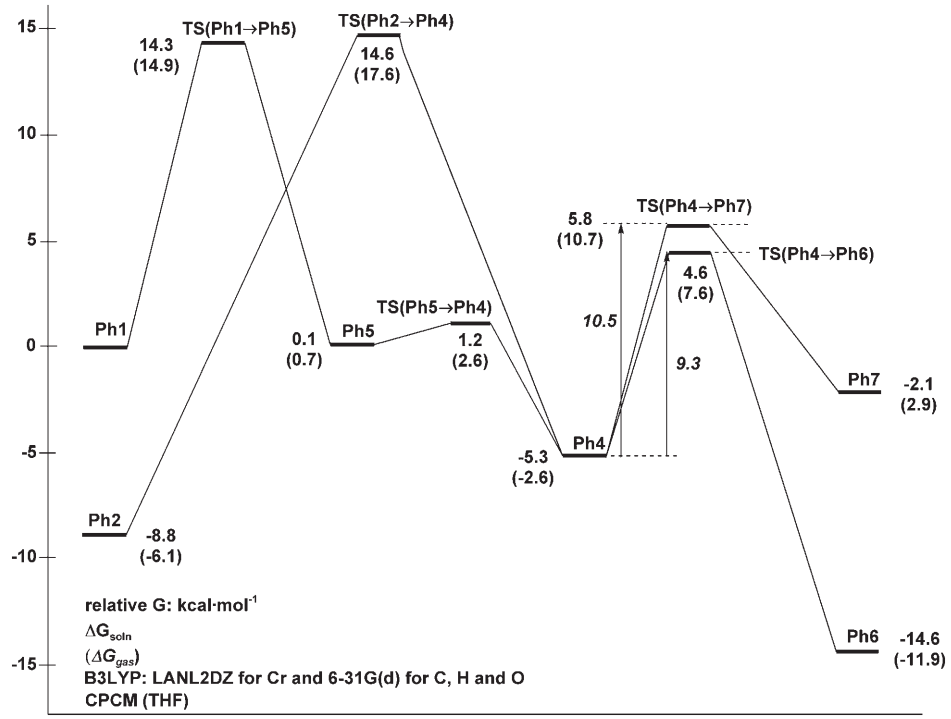

Figure 6. Gibbs energy profiles for system **Ph** in solution. Relative Gibbs energies in the gas phase are indicated in parentheses.

cipient six-membered ring. The structures of the transition states calculated for these transformations are very similar for the three systems. For instance, the bond distances for **TS(Ph4→Ph6)** (Figure 8) and **TS(In4→In6)** (Figure 11) match almost perfectly. Therefore, the substituent at C6 does not seem to influence the stability of these transition states.

On the other hand, the structures of the transition states that would lead to the formation of the cyclooctatrienones **Ph7** and **In7** are remarkably different, and thus, it must be expected that an analysis of their differences might explain their divergent reactivity.

During the transformation of **Ph4** to **Ph7** and **In4** to **In7**, two different events occur in a concerted manner: a conrotatory 8π-electron electrocyclic ring closure with C–C bond formation between C1 and C8 and the migration of $Cr(CO)_3$ from C1 to C6. For the indole-substituted system **In** we have found a very early transition state **TS(In4→In7)** with a very incipient bonding interaction between C1 and C8: d(C1–C8) = 2.67 Å. For system **TS(Ph4→Ph7)**, a much shorter distance is observed, d(C1–C8) = 2.06 Å, indicating a more advanced transition state. Moreover, the migration of the chromium atom is already highly developed in the phenyl-substituted system **TS(Ph4→Ph7)**, with very different distances between the chromium atom and C1 and C6: d(Cr–C1) = 2.93 Å and d(Cr–C6) = 2.41 Å. In contrast, $Cr(CO)_3$ migration is at the mid-point in **TS(In4→In7)**, as can be seen by the similar atomic distances: d(Cr–C1) = 2.58 Å and d(Cr–C6) = 2.52 Å. Therefore, for the **Ph** system, the aromaticity of the phenyl ring is already broken in the transition state and the energy cost associated with the aromaticity loss has to be paid to reach **TS(Ph4→Ph7)**. On the other hand, for the **In** system, the energy required to reach **TS(In4→In7)** is mostly paid in breaking the Cr–C1 interaction, whereas the loss of aromaticity of the indole does not influence the activation barrier because it occurs during the downhill part of the reaction. Clearly, the lower energy cost for the loss of aromaticity of the five-membered ring of the indole, when compared with the phenyl ring, is compensated by the incipient formation of the new C1–C8 bond and the stabilization of the metal by the new Cr–C6 interaction. Thereby, the different aromatic nature of the phenyl and indole rings determines the energy and the position of the transition state along the reaction coordinate. As a result, in the **Ph** model, the TS leading to the eight-membered ring, **TS(Ph4→Ph7)**, is destabilized when compared with the TS that leads to the benzannulation product, **TS(Ph4→Ph6)**. In contrast, in the **In** model, the transition state that leads to the cyclooctatrienone, **TS(In4→In7)**, is more stable and the eight-membered ring is the species that is formed.

From a thermodynamic point of view, the cyclooctatrienone **Ph7** is very unstable and its formation should proceed through an endergonic step. In contrast, cyclooctatrienone **In7** is the thermodynamically controlled product in the **In** reaction pathway. Again, the lack of aromaticity in **Ph7** is responsible for this dramatic difference in the energy profiles. In fact, in both models, **Ph** and **In**, the products obtained experimentally, **Ph6** and **In7**, respectively, are favoured by both kinetics and thermodynamics. Although thermodynamics may be important to justify the exclusive formation of **Ph6**, the formation of **In7** is successfully explained by employing kinetic arguments.

The computational study presented herein establishes a complex mechanistic picture with some alternative reaction pathways. As expected, the nature of the terminal substituent determines the lowest-energy reaction channel for each system. The preferred reaction channel found for the alkene-substituted system **A** consists of an unusual chelotropic-like reaction in which two C–C bonds are formed between a CO ligand and both ends of the carbon chain. However, this route does not operate in the aromatic-substituted systems. Instead, more conventional CO insertion–electrocyclization sequences have been identified. The different reactivities observed for the **Ph** and **In** systems rely on the dif-

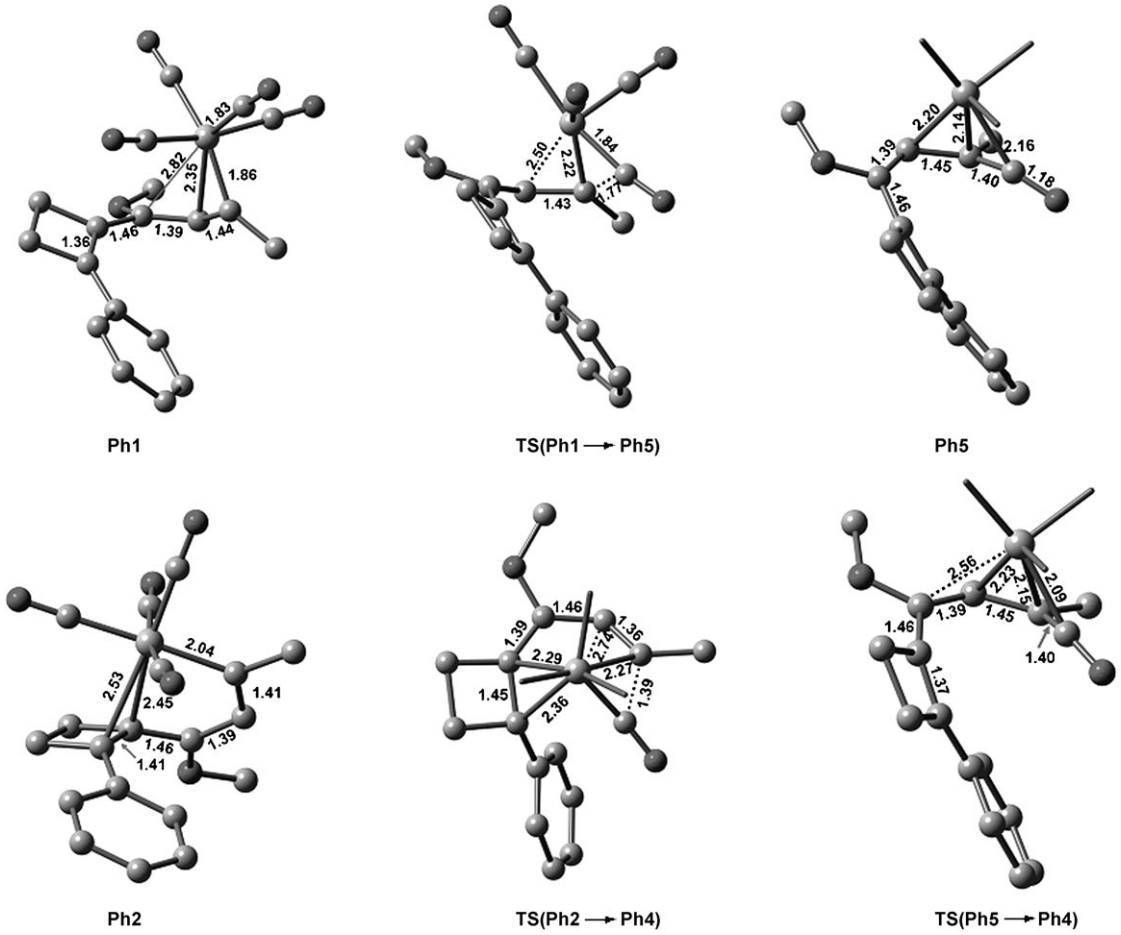

Figure 7. B3LYP-optimized structures for **Ph1**, **TS(Ph1→Ph5)**, **Ph5, TS(Ph5→Ph4)**, **Ph2** and **TS(Ph2→Ph4)**. Hydrogen atoms have been omitted for clarity. The CO ligands on the $Cr(CO)_3$ moiety have been omitted for clarity in **Ph5, TS(Ph5→Ph4)**, **Ph2** and **TS(Ph2→Ph4)**.

ferent structures found for the TS leading to the formation of the eight-membered ring system, which ultimately depends on the higher energetic cost required to break the aromaticity of the aromatic ring. Moreover, these results clearly establish the key role played by the $Cr(CO)_3$ fragment in the course of the electrocyclization reactions, and that could not have been anticipated in the absence of computational modelling.

Conclusion

In summary, in this paper we have reported a detailed experimental study of the extended Dötz reaction of cyclobutene-containing dienyl Fischer carbene complexes and alkynes, which represents a straightforward method for the preparation of cyclooctatrienones. The scope of this reaction includes metallahexa-1,3,5-trienes and also metallabuta-1,3-dienes with a benzo-fused heterocyclic substituent. Moreover, mechanisms for alternative reaction pathways, consistent with experimental results, have been established by means of DFT computations.

Experimental Section

General: All reactions were carried out under nitrogen. THF was distilled over benzophenone/sodium under nitrogen. Column chromatography was carried out on silica gel 60 (230–400 mesh). All other reagents were of the best commercial grade available. ^{1}H NMR spectra were recorded with a Bruker NAV-400 (400 MHz) or DPX-300 (300 MHz) spectrometer. Chemical shifts are reported in ppm from tetramethylsilane with the residual solvent resonance as the internal standard ($CHCl_3$: $\delta =$ 7.26 ppm). Data are reported as follows: chemical shift, multiplicity (s: singlet, d: doublet, dd: double doublet, td: triplet of doublets, t: triplet, q: quartet, br: broad, m: multiplet), coupling constants (J in Hz), integration and assignment. ^{13}C NMR spectra were recorded with a Bruker NAV-400 (100 MHz) or DPX-300 (75 MHz) spectrometer with complete proton decoupling. Chemical shifts are reported in ppm from tetramethylsilane with the solvent resonance as internal standard ($CDCl_3$: $\delta =$ 76.95 ppm). Two-dimensional NMR experiments (COSY, HMQC, HMBC and NOESY) were recorded with a Bruker AMX-400 (400 MHz) spectrometer. Electron-impact (EI) high-resolution mass spectrometry was carried out on a Finnigan-Mat 95 spectrometer.

General procedure for the preparation of alkynyl carbene complexes: These complexes were prepared from the corresponding acetylenes by the generation of the acetylide with BuLi in the presence of hexacarbonylchromium at −78 °C and then by allowing it to react by slowly increasing the temperature overnight. Carbene complexes **1** have already been described.[19a] Complexes **9, 10**, and **20** were prepared following the same standard methodology from the corresponding acetylenes. These acety-

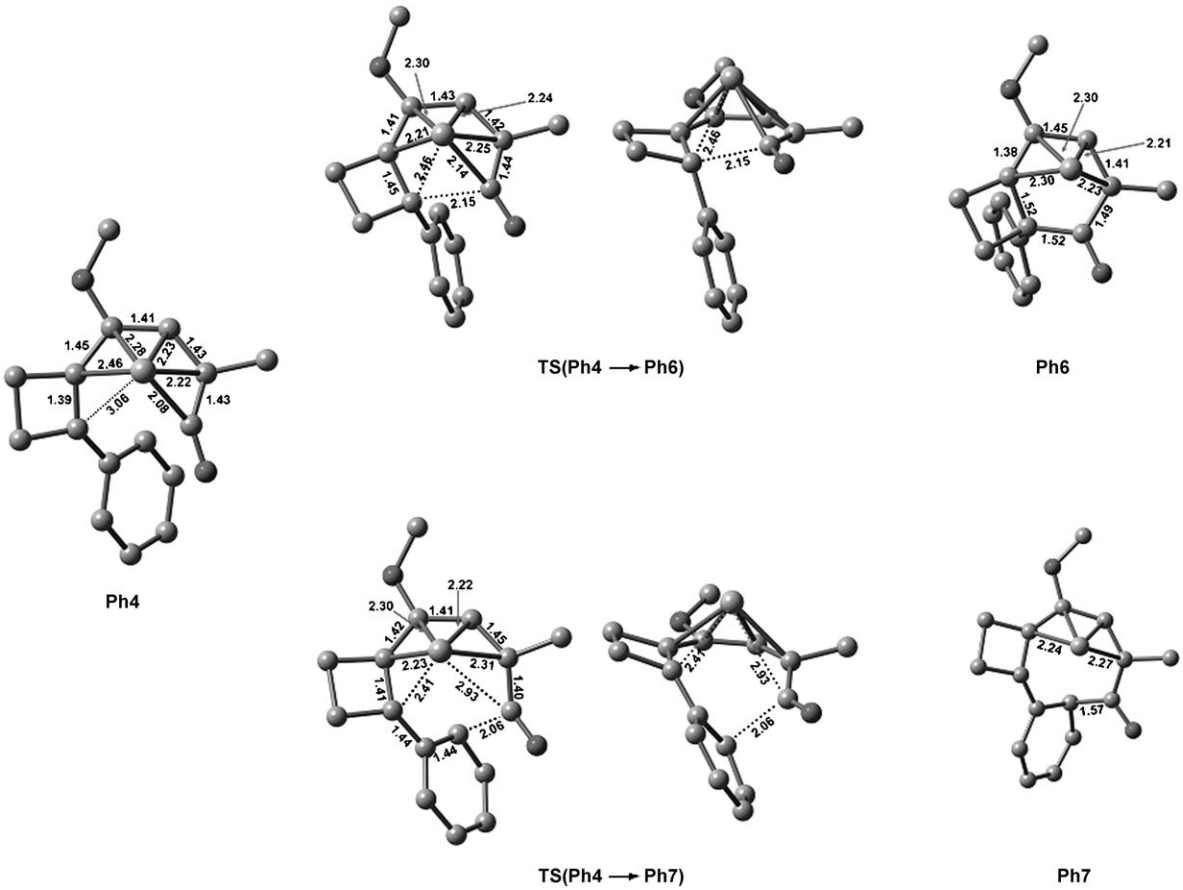

Figure 8. B3LYP-optimized structures for **Ph4**, **TS(Ph4→Ph6)**, **TS(Ph4→Ph7)**, **Ph6** and **Ph7**. Hydrogen atoms and the CO ligands on the $Cr(CO)_3$ moiety have been omitted for clarity.

lenes were prepared by Colvin rearrangement of the corresponding aldehydes by reaction with lithium trimethylsilyldiazomethane.[22]

Pentacarbonyl[1-methoxy-3-(1-methyl-1*H*-indol-3-yl)propynylidene]chromium(0) (9): Yield: 62%. Crystallized from hexane; violet crystals; ^{1}H NMR (300 MHz, $CDCl_3$): $\delta=7.72$ (d, $J=7.6$ Hz, 1H), 7.64 (s, 1H), 7.47–7.32 (m, 3H), 4.44 (s, 3H), 3.91 ppm (s, 3H); ^{13}C NMR (75 MHz, $CDCl_3$): $\delta=306.2$ (Cr=C), 225.2 (CO), 216.8 (4×CO), 138.3 (CH), 137.5 (C), 136.9 (C), 128.0 (C), 123.9 (CH), 122.6 (CH), 120.1 (CH), 110.3 (CH), 100.2 (C), 95.7 (C), 65.1 (OCH_3), 33.8 ppm (NCH_3).

Pentacarbonyl[1-methoxy-3-(1-methyl-1*H*-indol-2-yl)propynylidene]chromium(0) (10): Yield: 67%. Crystallized from hexane; violet crystals; ^{1}H NMR (300 MHz, $CDCl_3$): $\delta=7.54$ (d, $J=7.5$ Hz, 1H), 7.32–7.23 (m, 2H), 7.09–7.03 (m, 1H), 7.02 (s, 1H), 4.32 (s, 3H), 3.81 ppm (s, 3H); ^{13}C NMR (75 MHz, $CDCl_3$): $\delta=308.3$ (Cr=C), 225.2 (CO), 216.3 (4×CO), 139.8 (C), 127.4 (C), 126.0 (CH), 122.2 (CH), 121.0 (CH), 119.1 (C), 114.5 (CH), 110.0 (CH), 99.8 (C), 90.9 (C), 65.6 (OCH_3), 30.9 ppm (NCH_3).

Pentacarbonyl[1-methoxy-3-(benzo[*b*]furan-2-yl)propynylidene]chromium(0) (20): Yield: 67%. Crystallized from hexane; black crystals; ^{1}H NMR (400 MHz, $CDCl_3$): $\delta=7.68$ (d, $J=7.7$ Hz, 1H), 7.55–7.49 (m, 3H), 7.33 (t, $J=7.3$ Hz, 1H), 4.46 ppm (s, 3H); ^{13}C NMR (100 MHz, $CDCl_3$): $\delta=310.22$ (Cr=C), 225.6 (CO), 215.9 (4×CO), 156.4 (C), 128.3 (CH), 125.1 (C), 124.0 (CH), 123.1 (C), 122.1 (CH), 121.0 (CH), 111.9 (CH), 96.3 (C), 88.9 (C), 66.4 ppm (OCH_3).

General procedure for the preparation of dienyl carbene complexes: Complexes **2** and **4** have already been described.[19a] Complexes **6**, **7** and **8** were prepared following the same procedure by reaction of the neat carbene (1 mmol) with the corresponding enol ether (10 mmol) at room temperature under nitrogen.

Pentacarbonyl{methoxy[2,3,3a,5a-tetrahydro-4-(1-naphthyl)cyclobuta[*b*]-furan-5-yl]methylene}chromium(0) (6): Yield: 74%; orange solid; ^{1}H NMR (300 MHz, $CDCl_3$): $\delta=7.80$–7.76 (m, 2H), 7.62–7.59 (m, 1H), 7.45–7.39 (m, 4H), 5.67 (d, $J=3.5$ Hz, 1H), 4.19 (t, $J=8.8$ Hz, 1H), 4.16 (s, 3H), 4.10–4.02 (m, 1H), 3.78 (dd, $J=7.6$, 3.3 Hz, 1H), 1.88–1.69 ppm (m, 2H); ^{13}C NMR (100 MHz, $CDCl_3$): $\delta=335.8$ (Cr=C), 223.9 (CO), 216.3 (4×CO), 149.2 (C), 141.1 (C), 133.5 (C), 131.4 (C), 130.2 (CH), 129.9 (C), 128.8 (CH), 126.8 (2×CH), 126.2 (CH), 125.1 (CH), 125.0 (CH), 80.8 (OCH), 67.0 (OCH_2), 65.7 (OCH_3), 47.5 (CH), 27.0 ppm (CH_2).

Pentacarbonyl{methoxy[2,3,3a,5a-tetrahydro-4-(1-methyl-1*H*-indol-3-yl)-cyclobuta[*b*]furan-5-yl]methylene}chromium(0) (7): Yield: 78%; red solid; ^{1}H NMR (300 MHz, $CDCl_3$): $\delta=7.88$ (s, 1H), 7.82 (d, $J=7.3$ Hz, 1H), 7.46–7.28 (m, 3H), 5.84 (d, $J=3.7$ Hz, 1H), 4.81 (s, 3H), 4.20–4.13 (m, 1H), 3.98–3.81 (m, 2H), 3.87 (s, 3H), 2.16–2.07 ppm (m, 2H); ^{13}C NMR (75 MHz, $CDCl_3$): $\delta=320.2$ (Cr=C), 223.9 (CO), 217.1 (4×CO), 142.0 (C), 141.5 (C), 137.4 (C), 136.1 (CH), 127.7 (C), 123.3 (CH), 122.2 (CH), 121.0 (CH), 110.4 (CH), 110.3 (C), 81.3 (OCH), 65.8 (OCH_2), 64.6 (OCH_3), 45.4 (NCH_3), 33.7 (CH), 27.7 ppm (CH_2).

Pentacarbonyl{methoxy[2,3,3a,5a-tetrahydro-4-(1-methyl-1*H*-indol-2-yl)-cyclobuta[*b*]furan-5-yl]methylene}chromium(0) (8): Yield: 85%; red solid; ^{1}H NMR (300 MHz, $CDCl_3$): $\delta=7.60$ (d, $J=7.1$ Hz, 1H), 7.40–7.22 (m, 2H), 7.13 (br s, 1H), 6.80 (s, 1H), 5.74 (br s, 1H), 4.61 (s, 3H), 4.25–4.12 (m, 1H), 4.03–3.71 (m, 2H), 3.62 (s, 3H), 2.06–1.80 ppm (m, 2H); ^{13}C NMR (75 MHz, $CDCl_3$): $\delta=335.9$ (Cr=C), 223.8 (CO), 216.2 (4×CO), 145.9 (C), 139.6 (C), 133.0 (C), 130.4 (C), 127.3 (C), 124.4 (CH), 121.5 (CH), 120.6 (CH), 109.7 (CH), 108.2 (CH), 81.1 (OCH), 66.7 (OCH_2), 65.7 (OCH_3), 46.0 (NCH_3), 31.4 (CH), 27.5 ppm (CH_2).

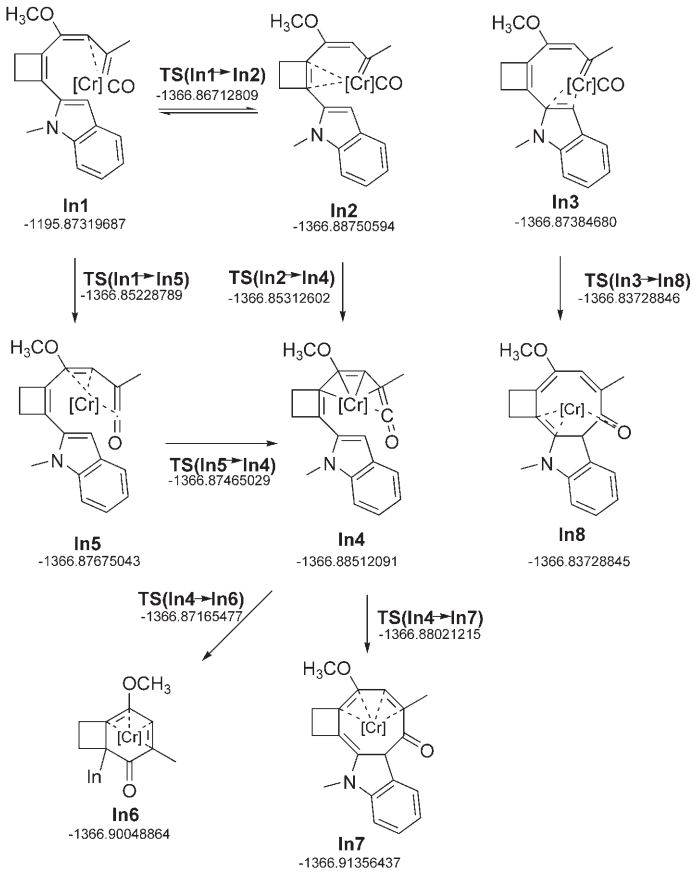

Figure 9. Reaction pathways found for system **In**. B3LYP electronic energies are indicated in hartrees.

General procedure for the preparation of carbocycles 3, 5, 15–19 and 21: A solution of the corresponding dienyl carbene (1 mmol) and acetylene (3 mmol) in THF (15 mL) was refluxed under nitrogen until TLC analysis revealed total consumption of the starting complex. The reaction mixture was diluted with hexane (20 mL) and exposed to sunlight and air in order to oxidise the metallic species to the corresponding organic compounds. Filtration through a pad of Celite and flash chromatography provided carbocycles **3, 5, 15–19**, or **21**.

One-pot process: The corresponding alkynyl carbene complex (0.5 mmol) was treated with the enol ether (2 mmol) in THF (10 mL) at room temperature for 10 h. Then the corresponding alkyne (2 mmol) was added and the mixture refluxed for 2 h. The oxidation and purification processes were carried out as described for the stepwise reaction.

Carbocycles **3a–e, 3j, 3m**, **5a**, and **5b** have already been described.[1]

1,2,3,3a,7b,9,10,10a-Octahydro-7-methoxy-5-trimethylsilylcyclopenta-[7′,8′]cycloocta[3,4]cyclobuta[*b*]furan-4-one (3f): A mixture of diastereoisomers. Yield: 55%; yellow oil; ^{1}H NMR (300 MHz, $CDCl_3$): δ=6.65 (s, 1H, maj.), 6.34 (s, 1H, min.), 5.40 (d, J=4.8 Hz, 1H, maj.), 5.09 (d, J=4.4 Hz, 1H, min.), 4.06–4.08 (m, 1H, min.), 4.00–4.01 (m, 1H, min.), 3.85 (s, 3H, maj.), 3.78 (s, 3H, min.), 3.56–3.63 (m, 1H, maj.), 3.32–3.40 (m, 1H, maj. + 1H, min.), 3.07–3.18 (m, 1H, min.), 2.51–2.61 (m, 2H), 2.30–2.42 (m, 10H), 1.81–2.11 (m, 16H), 0.17 ppm (s, 9H, maj. + 9H, min.); ^{13}C NMR (75 MHz, $CDCl_3$): δ=200.7 (C), 194.0 (C), 154.6 (C), 151.2 (C), 148.5 (C), 147.1 (C), 141.3 (C), 139.9 (C), 137.5 (CH, maj.), 132.5 (CH, min.), 132.4 (C), 132.0 (C), 127.4 (C), 126.3 (C), 79.7 (CH, maj.), 78.2 (CH, min.), 67.0 (CH_2, min.), 66.6 (CH_2, maj.), 59.8 (CH, min.), 58.7 (CH, maj.), 57.7 (CH_3, maj.), 57.6 (CH_3, min.), 45.2 (CH, min.), 45.2 (CH, maj.), 31.6 (CH_2, min.), 31.3 (CH_2, maj.), 29.5 (CH_2, min.), 29.5 (CH_2, maj.), 29.3 (CH_2, min.), 29.3 (CH_2, maj.), 26.5 (CH_2, maj.), 26.0 (CH_2, min.), −1.1 (CH_3, maj.), −1.5 ppm (CH_3, min.); HRMS (EI): m/z calcd for $C_{19}H_{26}O_3Si$: 330.1651; found: 330.1658.

7-Butyl-5,5a,9b,11,12,12a-hexahydro-3,3-dimethyl-9-methoxy-1*H*,3*H*-furo[2″,3″:3′,4′]cyclobuta[3,4]cycloocta[*e*][1,3]dioxepin-6-one (diast-3g): Major diastereoisomer. Yield: 51%; yellow oil; ^{1}H NMR (300 MHz, $CDCl_3$): δ=6.67 (s, 1H), 5.49 (d, J=4.8 Hz, 1H), 4.23 (d, J=14.8 Hz, 1H), 4.17 (d, J=14.8 Hz, 1H), 4.17–4.15 (m, 1H), 4.00 (t, J=8.3 Hz, 1H), 3.93 (s, 3H), 3.89 (dd, J=13.1, 4.3 Hz, 1H), 3.72 (dd, J=8.3, 4.8 Hz, 1H), 3.56–3.47 (m, 1H), 2.67–2.49 (m, 1H), 2.44–2.26 (m, 1H), 2.17–2.12 (m, 1H), 1.86–1.79 (m, 1H), 1.66–1.53 (m, 1H), 1.46 (s, 3H), 1.37 (s, 3H), 1.44–1.24 (m, 4H), 0.87 ppm (t, J=7.1 Hz, 3H); ^{13}C NMR (75 MHz, $CDCl_3$): δ=186.8 (C), 150.0 (C), 149.1 (C), 138.8 (C), 133.0 (CH), 127.2 (C), 123.5 (C), 101.9 (C), 80.9 (CH), 66.6 (CH_2), 60.2 (CH_2), 60.0 (CH_2), 58.1 (CH), 53.2 (CH_3), 44.9 (CH), 36.5 (CH_2), 32.1 (CH_2), 30.1 (CH_2), 24.4 (CH_3), 24.2 (CH_3), 22.4 (CH_2), 13.8 ppm (CH_3); elemental analysis calcd (%) for $C_{22}H_{30}O_5$: C 70.56, H 8.07; found: C 70.81, H 8.24.

7-Butyl-5,5a,9b,11,12,12a-hexahydro-3,3-dimethyl-9-methoxy-1*H*,3*H*-furo[2″,3″:3′,4′]cyclobuta[3,4]cycloocta[*e*][1,3]dioxepin-6-one (diast-3g): Minor diastereoisomer. Yield: 13%; yellow oil; ^{1}H NMR (300 MHz, $CDCl_3$): δ=6.61 (s, 1H), 5.31 (d, J=5.1 Hz, 1H), 4.24–4.10 (m, 4H), 3.99–3.97 (m, 1H), 3.94 (s, 1H), 3.87 (dd, J=13.1, 4.3 Hz, 1H), 3.62–3.57 (m, 1H), 2.58–2.41 (m, 2H), 2.35–2.18 (m, 1H), 2.16 (dd, J=10.8, 4.6 Hz, 1H), 1.92–1.77 (m, 1H), 1.46 (s, 3H), 1.38 (s, 3H), 1.47–0.93 (m, 4H), 0.89 ppm (t, J=7.1 Hz, 3H); ^{13}C NMR (75 MHz, $CDCl_3$): δ=190.1 (C), 151.3 (C), 150.8 (C), 141.6 (C), 130.8 (CH), 127.3 (C), 122.9 (C), 101.8 (C), 80.2 (CH), 67.5 (CH_2), 60.7 (CH_2), 60.1 (CH_2), 53.2 (CH_3), 45.5 (CH), 36.2 (CH_2), 31.8 (CH_2), 31.4 (CH_2), 24.9 (CH_3), 24.0 (CH_3), 22.5 (CH_2), 13.8 ppm (CH_3); elemental analysis calcd (%) for $C_{22}H_{30}O_5$: C 70.56, H 8.07; found: C 70.69, H 7.91.

8-Butyl-2,3,4,4a,6,10b-hexahydro-5-methyl-10-methoxy-6-phenyl-cycloocta[3,4]cyclobuta[*b*]pyran-7-one (3h): Yield: 77%; yellow oil; ^{1}H NMR (200 MHz, $CDCl_3$): δ=7.57–7.52 (m, 2H), 7.38–7.28 (m, 3H), 6.93 (s, 1H), 5.16 (d, J=6.7 Hz, 1H), 3.97 (s, 3H), 3.78 (td, J=5.3, 1.3 Hz, 2H), 3.26 (s, 1H), 2.71–2.60 (m, 1H), 2.52–2.38 (m, 1H), 2.12–2.01 (m, 1H), 1.62 (s, 3H), 1.50–1.32 (m, 8H), 0.90 ppm (t, J=7.1 Hz, 3H); ^{13}C NMR (50.3 MHz, $CDCl_3$): δ=183.1 (C), 150.6 (C), 148.8 (C), 140.3 (C), 136.3 (C), 132.8 (CH), 129.7 (2×CH), 128.8 (C), 128.0 (2×CH), 126.7 (CH), 126.0 (C), 71.6 (OCH), 62.5 (OCH_2), 59.5 (CH), 58.4 (OCH_3), 38.9 (CH), 36.7 (CH_2), 32.2 (CH_2), 23.3 (CH_2), 22.4 (CH_2), 20.5 (CH_2), 15.1 (CH_3), 13.8 ppm (CH_3).

7-Butyl-1,5,5a,9b,11,12,13,13a-octahydro-3,3-dimethyl-9-methoxy-3*H*-pyrano[2″,3″:3′,4′]cyclobuta[3,4]cycloocta[*e*][1,3]dioxepin-6-one (3i): Yield: 67%; yellow oil; ^{1}H NMR (300 MHz, $CDCl_3$): δ=6.83 (s, 1H), 5.06 (d, J=6.5 Hz, 1H), 4.17 (d, J=14.4 Hz, 1H), 4.07 (d, J=14.4 Hz, 1H), 3.89 (s, 3H), 3.96–3.75 (m, 2H), 3.74–3.52 (m, 2H), 3.33 (dd, J=12.6, 6.1 Hz, 1H), 2.62–2.53 (m, 1H), 2.48–2.28 (m, 1H), 2.19–2.17 (m, 1H), 2.01–1.93 (m, 1H), 1.44 (s, 3H), 1.38 (s, 3H), 1.51–1.23 (m, 5H), 0.86 (t, J=7.4 Hz, 3H), 0.95–0.80 ppm (m, 2H); ^{13}C NMR (75 MHz, $CDCl_3$): δ=186.9 (C), 149.5 (C), 149.3 (C), 139.9 (C), 133.2 (CH), 127.2 (C), 125.5 (C), 101.9 (C), 71.5 (OCH), 62.3 (OCH_2), 60.0 (CH_2), 58.2 (CH), 52.9 (OCH_3), 38.6 (CH), 36.4 (CH_2), 36.2 (CH_2), 32.2 (CH_2), 24.4 (CH_3), 24.1 (CH_3), 24.1 (CH_2), 22.4 (CH_2), 20.4 (CH_2), 13.8 ppm (CH_3); elemental analysis calcd (%) for $C_{23}H_{32}O_5$: C 71.11, H 8.30; found: C 71.35, H 8.08.

7-Butyl-5,5a,10,11-tetrahydro-3,3,10-trimethyl-9,10-dimethoxy-1*H*,3*H*-cyclobuta[3,4]cycloocta[*e*][1,3]dioxepin-6-one (3k): Yield: 56%; yellow oil; ^{1}H NMR (300 MHz, $CDCl_3$): δ=6.77 (s, 1H), 4.25–4.15 (m, 2H), 3.94–3.88 (m, 2H), 3.81 (s, 3H), 3.26 (s, 3H), 2.94 (d, J=3.1 Hz, 1H), 2.64–2.58 (m, 2H), 2.34–2.30 (m, 1H), 1.67 (s, 3H), 1.46 (s, 3H), 1.40 (s, 3H), 1.49–1.24 (m, 5H), 0.88 ppm (t, J=7.1 Hz, 3H); ^{13}C NMR (75 MHz, $CDCl_3$): δ=187.3 (C), 150.3 (C), 147.4 (C), 134.0 (C), 132.2 (CH), 130.8 (C), 129.5 (C), 101.9 (C), 81.4 (C), 60.9 (OCH_2), 60.0 (OCH_2), 59.5 (OCH_3), 53.5 (OCH_3), 51.3 (C), 36.9 (CH_2), 36.5 (CH_2), 32.1 (CH_2), 25.1 (CH_3), 24.6 (CH_3), 24.3 (CH_3), 22.6 (CH_2), 13.9 ppm (CH_3).

8-Butyl-6-methoxytricyclo[8.3.0.0^{2,5}]trideca-1(2),5,7-triene-4,9-dione (3l): Yield: 52%; yellow oil; ^{1}H NMR (200 MHz, $CDCl_3$): δ=6.73 (s, 1H), 4.19 (s, 3H), 3.43 (dd, J=15.9, 1.8 Hz, 1H), 3.29 (dd, J=15.9, 1.3 Hz, 1H), 2.79–2.74 (m, 1H), 2.66–2.16 (m, 6H), 1.95–1.69 (m, 2H), 1.52–1.21

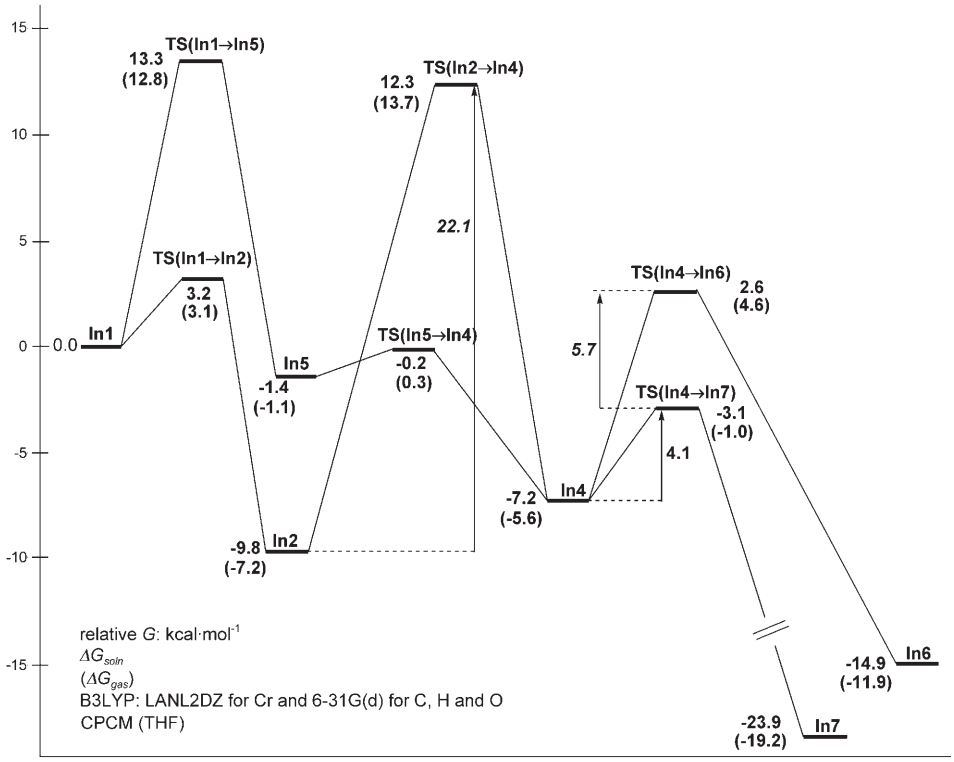

Figure 10. Gibbs energy profiles for system **In** in solution. Relative Gibbs energies in the gas phase are indicated in parentheses. The **In3** to **In8** transformation is not represented as a result of the high energy barrier involved.

(m, 4H), 0.91 ppm (t, $J=7.9$ Hz, 3H); ^{13}C NMR (75 MHz, $CDCl_3$): $\delta=$ 190.2 (C), 189.8 (C), 153.7 (C), 149.3 (C), 137.9 (C), 130.7 (CH), 128.3 (C), 126.7 (C), 61.8 (OCH_3), 57.3 (CH), 49.1 (CH_2), 37.4 (CH_2), 31.7 (CH_2), 31.6 (CH_2), 28.0 (CH_2), 25.9 (CH_2), 22.5 (CH_2), 13.8 ppm (CH_3); HRMS (EI): m/z calcd for $C_{18}H_{22}O_3$: 286.1569; found: 286.1573.

7-Butyl-5,5a,10,11-tetrahydro-3,3-dimethyl-9,10,10,11,11-pentamethoxy-1*H*,3*H*-cyclobuta[3,4]cycloocta[*e*][1,3]dioxepin-6-one (3n): Yield: 60%; yellow oil; ^{1}H NMR (300 MHz, $CDCl_3$): $\delta=6.83$ (s, 1H), 4.78 (d, $J=$ 14.2 Hz, 1H), 4.17–4.08 (m, 2H), 3.96 (dd, $J=12.8$, 3.0 Hz, 1H), 3.78 (s, 3H), 3.51 (s, 3H), 3.49 (s, 3H), 3.42 (s, 3H), 3.11 (s, 3H), 2.67–2.58 (m, 1H), 2.41–2.31 (m, 1H), 2.19–2.17 (m, 1H), 1.44 (s, 3H), 1.40 (s, 3H), 1.37–1.19 (m, 4H), 0.87 ppm (t, $J=7.1$ Hz, 3H); ^{13}C NMR (75 MHz, $CDCl_3$): $\delta=186.8$ (C), 153.7 (C), 148.9 (C), 137.2 (C), 135.9 (C), 131.0 (CH), 128.0 (C), 107.8 (C), 107.0 (C), 102.1 (C), 60.7 (OCH_2), 59.8 (OCH_2), 58.2 (OCH_3), 54.1 (CH), 53.4 (OCH_3), 52.1 (OCH_3), 51.9 (OCH_3), 51.7 (OCH_3), 36.6 (CH_2), 32.1 (CH_2), 24.5 (CH_3), 23.9 (CH_3), 22.5 (CH_2), 13.8 ppm (CH_3).

1,2,3,3a,7b,9,10,10a-Octahydro-7-methoxy-5,6-diphenylcyclopenta[7′,8′]-cycloocta[3,4]cyclobuta[*b*]furan-4-one (3o): Yield: 38%; yellow solid; ^{1}H NMR (300 MHz, $CDCl_3$): $\delta=7.18$–7.10 (m, 8H), 6.95–6.92 (m, 2H), 5.17 (d, $J=5.4$ Hz, 1H), 4.26–4.20 (m, 1H), 4.11 (c, $J=8.5$ Hz, 1H), 3.54–3.39 (m, 1H), 3.38 (s, 3H), 3.37–3.26 (m, 1H), 2.48–2.39 (m, 1H), 2.30–2.16 (m, 1H), 2.05–1.85 (m, 4H), 1.60–1.45 ppm (m, 2H); ^{13}C NMR (75 MHz, $CDCl_3$): $\delta=209.4$ (C), 149.9 (C), 147.0 (C), 138.4 (C), 136.2 (C), 134.6 (C), 133.1 (C), 130.8 (2×CH), 130.1 (2×CH), 128.5 (C), 128.5 (2×CH), 128.1 (CH), 127.9 (2×CH), 127.6 (CH), 127.1 (C), 78.1 (OCH), 66.7 (OCH_2), 58.1 (CH), 56.5 (OCH_3), 46.0 (CH), 30.3 (CH_2), 30.2 (CH_2), 29.0 (CH_2), 22.3 ppm (CH_2); elemental analysis calcd (%) for $C_{28}H_{26}O_3$: C 81.92, H 6.38; found: C 82.11, H 6.69. HRMS (EI): m/z calcd for $C_{28}H_{26}O_3$: 410.1882; found: 410.1888.

5-Butyl-2,3,3a,7b-tetrahydro-3b-(1-naphthyl)-7-methoxy-3b*H*-benzo-[3,4]cyclobuta[*b*]furan-4-one (5c): Yield: 52%; yellow solid; ^{1}H NMR (400 MHz, $CDCl_3$): $\delta=8.48$ (d, $J=$ 8.6 Hz, 1H), 7.98 (dd, $J=7.2$, 1.0 Hz, 1H), 7.87 (d, $J=8.2$ Hz, 1H), 7.79 (d, $J=8.1$ Hz, 1H), 7.58 (ddd, $J=8.6$, 6.9, 1.3 Hz, 1H), 7.48 (ddd, $J=7.9$, 6.9, 1.0 Hz, 1H), 7.42 (t, $J=8.0$ Hz, 1H), 6.30 (s, 1H), 5.26 (d, $J=5.9$ Hz, 1H), 4.17 (t, $J=8.4$ Hz, 1H), 4.05 (s, 3H), 3.86 (ddd, $J=11.3$, 9.0, 5.7 Hz, 1H), 3.56 (dd, $J=8.8$, 5.9 Hz, 1H), 2.80 (dd, $J=13.2$, 5.7 Hz, 1H), 2.13–2.07 (m, 2H), 1.91–1.87 (m, 1H), 0.99–0.86 (m, 4H), 0.57 ppm (t, $J=6.9$ Hz, 1H); ^{13}C NMR (100 MHz, $CDCl_3$): $\delta=204.2$ (CO), 148.9 (C), 140.7 (C), 135.0 (C), 133.2 (CH), 132.3 (C), 130.7 (C), 129.2 (CH), 129.0 (CH), 126.0 (CH), 125.9 (CH), 125.6 (CH), 125.0 (CH), 124.3 (CH), 113.9 (CH), 79.3 (OCH), 67.0 (OCH_2), 58.0 (OCH_3), 57.3 (C), 48.6 (CH), 29.8 (CH_2), 29.0 (CH_2), 26.8 (CH_2), 21.7 (CH_2), 13.5 ppm (CH_3); HRMS (EI): m/z calcd for $C_{25}H_{26}O_3$: 374.1882; found: 374.1885.

6-Butyl-1,2,3a,6,8,12d-hexahydro-4-methoxy-8-methylfuro[2″,3″:3′,4′]-cyclobuta[3,4]cyclooct[*b*]indol-7-one (15a): Yield: 50%; yellow oil; ^{1}H NMR (300 MHz, $CDCl_3$): $\delta=7.87$ (d, $J=8.2$ Hz, 1H), 7.33 (d, $J=3.5$ Hz, 2H), 7.16–7.11 (m, 1H), 5.46 (dt, $J=$ 7.0, 1.3 Hz, 1H), 5.15, (d, $J=3.1$ Hz, 1H), 4.09–4.02 (m, 3H), 3.84 (s, 3H), 3.85–3.83 (m, 1H), 3.22 (s, 3H), 2.30–2.23 (m, 1H), 2.20–2.10 (m, 1H), 1.81–1.64 (m, 2H), 1.17–1.02 (m, 2H), 0.89–0.70 (m, 2H), 0.64 ppm (t, $J=7.0$ Hz, 3H); ^{13}C NMR (75 MHz, $CDCl_3$): $\delta=196.4$ (CO), 140.8, 139.9, 138.8, 137.4, 136.3, 134.3, 126.0 (CH), 124.7, 122.1 (CH), 121.4 (CH), 114.9, 110.5 (CH), 79.3 (OCH), 75.1 (*C*HCO), (66.4 (OCH_2), 56.6 (OCH_3), 47.3 (NCH_3), 34.2 (CH_2), 32.2 (CH), 30.8 (CH_2), 26.9 (CH_2), 21.9 (CH_2), 13.6 ppm (CH_3); HRMS (EI): m/z calcd for $C_{24}H_{27}O_3N$: 377.1985; found: 377.1995.

1,2,3a,6,8,12d-Hexahydro-4-methoxy-8-methyl-6-octylfuro[2″,3″:3′,4′]-cyclobuta[3,4]cyclooct[*b*]indol-7-one (15b): Yield: 49%; yellow oil; ^{1}H NMR (300 MHz, $CDCl_3$): $\delta=8.03$ (d, $J=8.2$ Hz, 1H), 7.47 (d, $J=3.6$ Hz, 2H), 7.31–7.26 (m, 1H), 5.62 (d, $J=7.0$ Hz, 1H), 5.30 (d, $J=3.1$ Hz, 1H), 4.25–4.18 (m, 3H), 4.00 (s, 3H), 3.99–3.91 (m, 1H), 3.38 (s, 3H), 2.50–2.41 (m, 1H), 2.34–2.25 (m, 1H), 1.97–1.82 (m, 2H), 1.40–1.25 (m, 4H), 1.25–1.02 (m, 6H), 0.84 ppm (t, $J=6.7$ Hz, 3H); ^{13}C NMR (75 MHz, $CDCl_3$): $\delta=196.4$ (CO), 140.7, 138.7, 137.3, 136.2, 134.3, 126.6, 125.9 (CH), 124.6, 122.0 (CH), 121.4 (CH), 114.9, 110.4 (CH), 79.3 (OCH), 75.0 (*C*HCO), 66.4 (OCH_2), 56.6 (OCH_3), 47.2 (NCH_3), 34.7 (CH_2), 32.2 (CH), 31.5 (CH_2), 29.0 (CH_2), 28.9 (CH_2), 28.7 (CH_2), 28.6 (CH_2), 26.9 (CH_2), 22.4 (CH_2), 13.9 ppm (CH_3); HRMS (EI): m/z calcd for $C_{28}H_{35}O_3N$: 433.2611; found: 433.2614.

1,2,3a,6,8,12d-Hexahydro-4-methoxy-8-methyl-6-(2-phenylethyl)furo-[2″,3″:3′,4′]cyclobuta[3,4]cyclooct[*b*]indol-7-one (15c): Yield: 57%; yellow oil; ^{1}H NMR (300 MHz, $CDCl_3$): $\delta=7.87$ (dd, $J=8.2$, 0.8 Hz, 1H), 7.35–7.32 (m, 2H), 7.18–7.12 (m, 3H), 6.94–6.91 (m, 3H), 6.79–6.76 (m, 2H), 5.46 (d, $J=6.9$ Hz, 1H), 5.12 (d, $J=2.8$ Hz, 1H), 4.05–3.97 (m, 3H), 3.78 (s, 3H), 3.70–3.60 (m, 1H), 3.19 (s, 3H), 2.64–2.50 (m, 4H), 1.76–1.70 ppm (m, 2H); ^{13}C NMR (75 MHz, $CDCl_3$): $\delta=195.7$ (CO), 140.3 (C), 138.8 (C), 136.3 (C), 136.1 (C), 134.4 (C), 128.4 (C), 128.2 (CH), 128.0 (CH), 126.0 (CH), 125.8 (CH), 124.7 (C), 122.1 (CH), 121.4 (CH), 115.2 (C), 110.5 (CH), 79.2 (OCH), 74.9 (*C*HCO), 66.4 (OCH_2), 56.6

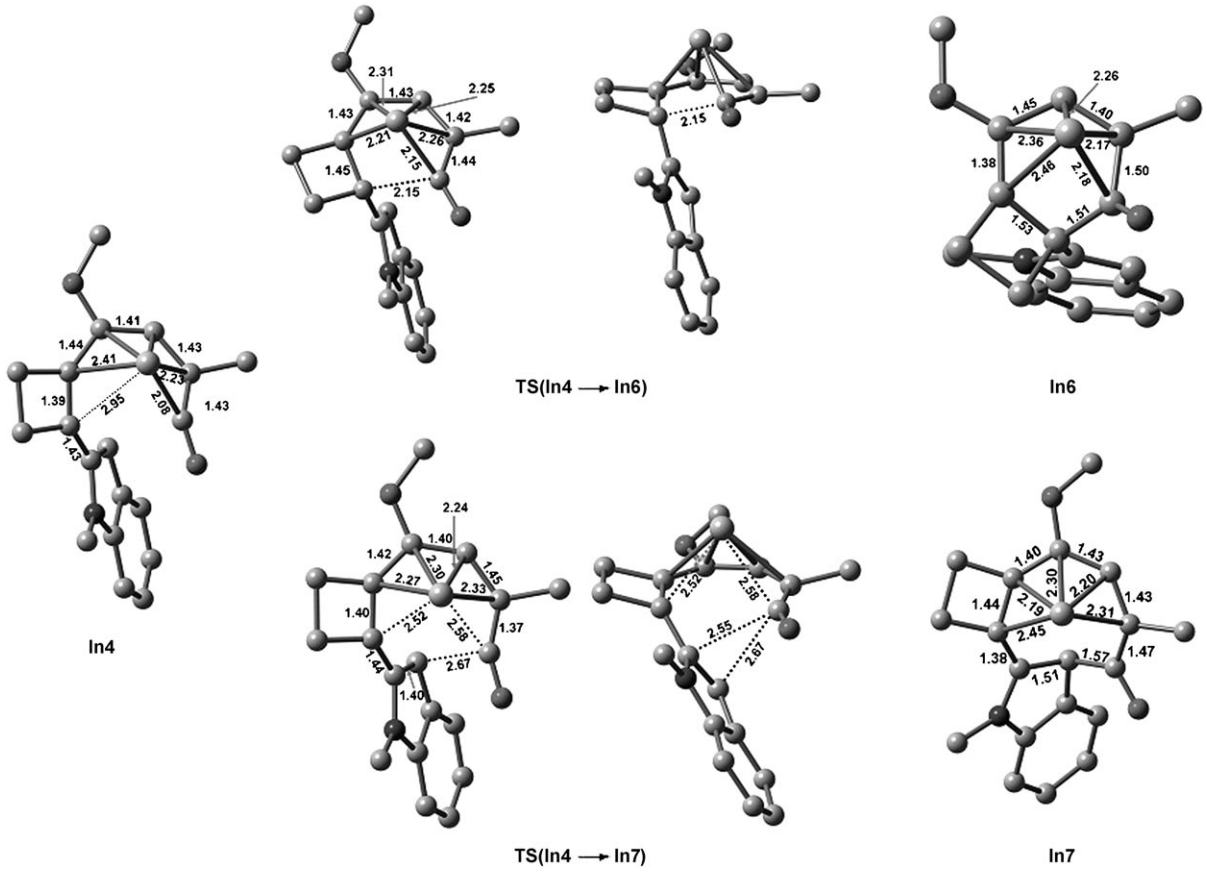

Figure 11. B3LYP-optimized structures for **In4, TS(In4→In6)**, **TS(In4→In7)**, **In6** and **In7**. Hydrogen atoms and the CO ligands on the chromium atom have been omitted for clarity.

(OCH_3), 47.3 (NCH_3), 36.4 (CH_2), 35.3 (CH_2), 32.3 (CH), 26.9 ppm (CH_2); HRMS (EI): *m*/*z* calcd for $C_{28}H_{27}O_3N$: 425.1985; found: 425.1994.

(3a*R,6*S**,12c*R**)-6-Butyl-1,2,3a,6,12,12c-hexahydro-4-methoxy-12-methylfuro[3″,2″:3′,4′]cyclobuta[7,8]cyclooct[*b*]indol-7-one (16a)**: Yield: 58%; yellow solid; m.p. 151–153°C; ^{1}H NMR (300 MHz, $CDCl_3$): δ = 8.70 (d, J = 8.0 Hz, 1H), 7.44–7.42 (m, 2H), 7.37–7.32 (m, 1H), 5.48 (d, J = 3.5 Hz, 1H), 4.73 (d, J = 8.8 Hz, 1H), 4.39–4.35 (m, 1H), 4.32–4.26 (m, 1H), 4.05 (s, 3H), 3.84 (dd, J = 16.6, 9.1 Hz, 1H), 3.64 (s, 3H), 2.63–2.55 (m, 1H), 2.27–2.13 (m, 1H), 2.06–1.91 (m, 3H), 1.42–1.27 (m, 4H), 0.92 ppm (t, J = 6.7 Hz, 3H); ^{13}C NMR (75 MHz, $CDCl_3$): δ = 191.7 (CO), 150.4 (C), 141.3 (C), 137.0 (C), 135.8 (C), 134.2 (C), 127.5 (C), 124.8 (CH), 123.1 (CH), 122.5 (CH), 122.0 (C), 109.1 (CH), 108.3 (CH), 78.2 (OCH), 66.8 (OCH_2), 55.4 (OCH_3), 48.8 (NCH_3), 48.4 (*C*HCO), 32.5 (CH), 29.9 (CH_2), 29.8 (CH_2), 27.5 (CH_2), 22.6 (CH_2), 13.9 ppm (CH_3); HRMS (EI): *m*/*z* calcd for $C_{24}H_{27}O_3N$: 377.1985; found: 377.1989.

(3a*R,6*R**,12c*R**)-1,2,3a,6,12,12c-Hexahydro-4-methoxy-12-methyl-6-phenylfuro[3″,2″:3′,4′]cyclobuta[7,8]cyclooct[*b*]indol-7-one (16b)**: Yield: 63%; yellow oil; ^{1}H NMR (300 MHz, $CDCl_3$): δ = 8.50 (d, J = 8.1 Hz, 1H), 7.34–7.23 (m, 6H), 7.21–7.12 (m, 3H), 5.37 (d, J = 3.5 Hz, 1H), 5.13 (d, J = 9.2 Hz, 1H), 4.30–4.26 (m, 1H), 4.19–4.13 (m, 1H), 3.94 (s, 3H), 3.81 (d, J = 9.2 Hz, 1H), 3.82–3.73 (m, 1H), 3.53 (s, 3H), 1.91–1.78 ppm (m, 2H); ^{13}C NMR (75 MHz, $CDCl_3$): δ = 188.9 (CO), 150.7 (C), 141.1 (C), 138.7 (C), 137.0 (C), 135.8 (C), 134.9 (C), 129.1 (CH), 128.2 (CH), 127.7 (C), 127.0 (CH), 125.0 (CH), 123.2 (CH), 122.6 (CH), 121.8 (C), 109.1 (CH), 107.3 (CH), 78.3 (OCH), 66.9 (OCH_2), 55.5 (OCH_3), 54.3 (*C*HCO), 48.9 (NCH_3), 32.5 (CH), 27.5 ppm (CH_2); HRMS (EI): *m*/*z* calcd for $C_{26}H_{23}O_3N$: 397.1672; found: 397.1676.

(3a*R,6*S**,12c*R**)-6-Benzyl-1,2,3a,6,12,12c-hexahydro-4-methoxy-12-methylfuro[3″,2″:3′,4′]cyclobuta[7,8]cyclooct[*b*]indol-7-one (16c)**: Yield: 68%; orange solid; m.p. 211–214°C; ^{1}H NMR (400 MHz, $CDCl_3$): δ = 8.67 (d, J = 8.0 Hz, 1H), 7.39–7.29 (m, 4H), 7.24–7.13 (m, 4H), 5.40 (d, J = 3.5 Hz, 1H), 4.80 (d, J = 8.8 Hz, 1H), 4.30 (dd, J = 8.4, 3.5 Hz 1H), 4.18–4.13 (m, 1H), 3.99 (s, 3H), 3.69–3.59 (m, 2H), 3.58 (s, 3H), 3.23 (dd, J = 15.0, 7.6 Hz, 1H), 2.88 (dd, J = 15.0, 7.4 Hz, 1H), 1.90–1.85 ppm (m, 2H); ^{13}C NMR (75 MHz, $CDCl_3$): δ = 190.8 (CO), 150.5 (C), 141.2 (C), 140.2 (C), 137.0 (C), 135.8 (C), 134.4 (C), 128.8 (CH), 128.2 (CH), 127.7 (C), 125.9 (CH), 124.9 (CH), 123.0 (CH), 122.5 (CH), 121.6 (C), 109.1 (CH), 107.6 (CH), 78.1 (OCH), 66.6 (OCH_2), 55.4 (OCH_3), 50.2 (*C*HCO), 48.8 (NCH_3), 36.2 (CH_2), 32.4 (CH), 27.4 ppm (CH_2); HRMS (EI): *m*/*z* calcd for $C_{27}H_{25}O_3N$: 411.1828; found: 411.1827.

(3a*R,6*S**,12c*R**)-1,2,3a,6,12,12c-Hexahydro-4-methoxy-12-methyl-6-(2-phenylethyl)furo[3″,2″:3′,4′]cyclobuta[7,8]cyclooct[*b*]indol-7-one (16d)**: Yield: 70%; yellow solid; m.p. 200–202°C; ^{1}H NMR (400 MHz, $CDCl_3$): δ = 8.62 (d, J = 8.1 Hz, 1H), 7.31–7.22 (m, 3H), 7.07–7.00 (m, 3H), 6.93–6.90 (m, 2H), 5.26 (d, J = 3.5 Hz, 1H), 4.61 (d, J = 8.8 Hz, 1H), 4.13 (dd, J = 7.7, 3.5 Hz, 1H), 3.87 (s, 3H), 3.85 (dd, J = 9.6, 7.5 Hz, 1H), 3.47 (s, 3H), 3.01 (ddd, J = 11.1, 9.6, 5.3 Hz, 1H), 2.72–2.49 (m, 3H), 2.40 (td, J = 8.4, 5.9 Hz, 1H), 2.08–1.97 (m, 1H), 1.64 (dddd, J = 12.7, 11.1, 7.7, 7.5 Hz, 1H), 1.58 ppm (dd, J = 12.7, 5.3 Hz, 1H); ^{13}C NMR (100 MHz, $CDCl_3$): δ = 191.2 (CO), 150.4 (C), 141.6 (C), 141.2 (C), 136.9 (C), 135.8 (C), 134.3 (C), 128.4 (CH), 128.0 (CH), 127.5 (C), 125.5 (CH), 124.8 (CH), 123.1 (CH), 122.5 (CH), 121.8 (C), 109.1 (CH), 107.4 (CH), 78.0 (OCH), 66.6 (OCH_2), 55.3 (OCH_3), 48.7 (NCH_3), 46.6 (*C*HCO), 33.2 (CH_2), 32.4 (CH), 31.5 (CH_2), 27.2 ppm (CH_2); HRMS (EI): *m*/*z* calcd for $C_{28}H_{27}O_3N$: 425.1985; found: 425.1986.

X-ray diffraction study of 16d: Data collection, crystal and refinement parameters are collected in Table 3. Data collection was performed at 293(2) K on a Nonius-Kappa CCD single-crystal diffractometer using $Cu_{K\alpha}$ radiation (λ = 1.5418 Å). Images were collected at a 29 mm fixed crystal–detector distance using the oscillation method with 2° oscillation

Table 3. Crystal data and structure refinement parameters for **16d**.

	16d
empirical formula	$C_{28}H_{27}O_3N$
formula weight	425.51
temperature [K]	293(2)
wavelength [Å]	1.5418
crystal system	monoclinic
space group	$P21/c$
unit cell dimensions	
a [Å]	12.5300(3)
b [Å]	10.7140(2)
c [Å]	20.1690(3)
α [°]	90
β [°]	125.522(1)
γ [°]	90
volume [Å^3]	2203.71(7)
Z	4
ρ_{calcd} [Mg m^{-3}]	1.283
μ [mm^{-1}]	0.657
$F(000)$	904
crystal size [mm^3]	0.20×0.17×0.07
θ range for data collection [°]	4.34–67.87
index ranges	
	$-14 \leqq h \leqq 14$
	$-12 \leqq k \leqq 0$
	$-24 \leqq l \leqq 13$
reflections collected	28931
independent reflections	3882 [R(int) = 0.0503]
completeness to θ [°]	67.87 (97.0%)
absorption correction	semi-empirical from equivalents
max. and min. transmission	1.043 and 0.970
refinement method	full-matrix least-squares on F^2
data/restraints/parameters	3882/0/398
goodness-of-fit on F^2	1.066
final R indices [$I>2\sigma(I)$]	R_1 = 0.0375, wR_2 = 0.0948
R indices (all data)	R_1 = 0.0505, wR_2 = 0.1043
extinction coefficient	0.0049(5)
largest diff. peak and hole [e Å^{-3}]	0.172 and −0.132

and a 70 s exposure time per image. The data collection strategy was calculated with the program Collect, Nonius BV, 1997–2004. Data reduction and cell refinement were performed with the HKL Denzo and Scalepack programs.[28] Unit cell dimensions were determined from 3756 reflections between θ = 2 and 70°. Multiple observations were averaged, R_{merge} = 0.050, resulting in 3882 unique reflections of which 3028 were observed with $I>2\sigma(I)$. A semiempirical absorption correction was applied using the SORTAV program.[29] The crystal structure was solved by direct methods using the SIR-92 program.[30] Anisotropic least-squares refinement was carried out with SHELXL-97.[31] All non-hydrogen atoms were anisotropically refined. All hydrogen atoms were located on a difference Fourier map and isotropically refined. The final cycle of full-matrix least-squares refinement based on 3882 reflections and 398 parameters converged to a final value of R_1 [$F^2>2\sigma(F^2)$] = 0.0375, wR_2 [$F^2>2\sigma(F^2)$] = 0.0948, $R_1(F^2)$ = 0.0505, $wR_2(F^2)$ = 0.1043. Final difference Fourier maps showed no peaks higher than 0.172 e Å^{-3} nor deeper than −0.132 e Å^{-3}. CCDC-639747 contains the supplementary data for this paper. These data can be obtained free of charge from The Cambridge Crystallographic Data Centre via www.ccdc.cam.ac.uk/data_request/cif.

1,2,3a,6,12,12c-Hexahydro-4-methoxy-12-methyl-6-(1-methylethylidene)furo[3″,2″:3′,4′]cyclobuta[7,8]cycloocta[*b*]indol-7-one (17): Yield: 62%; orange solid; m.p. 235–237 °C; ^{1}H NMR (300 MHz, $CDCl_3$): δ = 8.61 (d, J = 7.8 Hz, 1H), 7.31–7.18 (m, 3H), 5.29 (brs, 1H), 5.25 (d, J = 3.5 Hz, 1H), 4.09 (dd, J = 7.4, 3.4 Hz, 1H), 3.99 (dd, J = 7.4, 7.1 Hz, 1H), 3.81 (s, 3H), 3.55 (s, 3H), 3.52–3.46 (m, 1H), 1.69–1.56 (m, 2H), 1.60 (d, J = 1.4 Hz, 3H), 1.44 ppm (d, J = 1.9 Hz, 3H); ^{13}C NMR (75 MHz, $CDCl_3$): δ = 191.7 (CO), 151.1 (C), 141.7 (C), 137.3 (C), 136.9 (C), 132.9 (C), 132.7 (C), 132.2 (C), 127.5 (C), 124.7 (CH), 123.3 (CH), 122.6 (CH), 122.3 (C), 109.1 (CH), 103.0 (CH), 78.2 (OCH), 66.3 (OCH_2), 55.5 (OCH_3), 48.7 (NCH_3), 32.3 (CH), 27.1 (CH_2), 20.5 (CH_3), 20.2 ppm (CH_3); HRMS (EI): m/z calcd for $C_{23}H_{23}O_3N$: 361.1672; found: 361.1674.

2,3,3a,7b-Tetrahydro-3b-(1-methyl-1*H*-indol-3-yl)-7-methoxy-5-trimethylsilyl-3b*H*-benzo[3,4]cyclobuta[*b*]furan-4-one (18a): Yield: 48%; yellow oil; ^{1}H NMR (300 MHz, $CDCl_3$): δ = 7.83 (d, J = 8.0 Hz, 1H), 7.30–7.19 (m, 2H), 7.12 (d, J = 7.8 Hz, 1H), 7.10 (s, 1H), 6.67 (s, 1H), 5.46 (d, J = 5.8 Hz, 1H), 4.13 (d, J = 8.5 Hz, 1H), 4.01 (s, 3H), 3.82–3.73 (m, 1H), 3.76 (s, 3H), 3.39 (dd, J = 8.4, 5.8 Hz, 1H), 2.53 (dd, J = 13.4, 5.9 Hz, 1H), 2.02–1.96 (m, 1H), −0.05 ppm (s, 9H); ^{13}C NMR (75 MHz, $CDCl_3$): δ = 206.2 (CO), 146.9 (C), 144.8 (CH), 142.6 (C), 137.8 (C), 126.2 (CH), 126.0 (C), 121.7 (CH), 120.6 (CH), 119.2 (CH), 118.5 (C), 111.3 (C), 109.3 (CH), 80.6 (OCH), 67.5 (OCH_2), 57.8 (OCH_3), 51.7 (C), 48.2 (NCH_3), 32.7 (CH), 26.7 (CH_2), −1.7 ppm (3×CH_3).

5-*tert*-Butyl-2,3,3a,7b-tetrahydro-3b-(1-methyl-1*H*-indol-3-yl)-7-methoxy-3b*H*-benzo[3,4]cyclobuta[*b*]furan-4-one (18b): Yield: 52%; yellow solid; m.p. 149–153 °C; ^{1}H NMR (300 MHz, $CDCl_3$): δ = 7.81 (d, J = 7.9 Hz, 1H), 7.28 (d, J = 8.1 Hz, 1H), 7.20 (t, J = 7.0 Hz, 1H),7.10 (t, J = 7.1 Hz, 1H), 7.10 (s, 1H), 6.29 (s, 1H), 5.37 (d, J = 5.7 Hz, 1H), 4.10 (t, J = 8.4 Hz, 1H), 4.01 (s, 3H), 3.86–3.76 (m, 1H), 3.73 (s, 3H), 3.35 (dd, J = 8.8, 5.7 Hz, 1H), 2.57 (dd, J = 13.4, 5.8 Hz, 1H), 1.96 (m, 1H), 0.93 ppm (s, 9H); ^{13}C NMR (75 MHz, $CDCl_3$): δ = 203.5 (CO), 147.9 (C), 146.9 (C), 137.8 (C), 131.5 (CH), 126.4 (CH), 126.0 (C), 121.6 (CH), 120.5 (CH), 119.2 (CH), 114.3 (C), 111.0 (C), 109.3 (CH), 79.7 (OCH), 67.3 (OCH_2), 57.7 (OCH_3), 52.1 (C), 47.4 (NCH_3), 34.3 (C), 32.6 (CH), 29.0 (3×CH_3), 26.7 ppm (CH_2); HRMS (EI): m/z calcd for $C_{24}H_{27}O_3N$: 377.1985; found: 377.1980.

5-*tert*-Butyl-2,3,3a,7b-tetrahydro-3b-(1-methyl-1*H*-indol-2-yl)-7-methoxy-3b*H*-benzo[3,4]cyclobuta[*b*]furan-4-one (19): Yield: 43%; yellow solid; m.p. 155–158 °C; ^{1}H NMR (400 MHz, $CDCl_3$): δ = 7.56 (d, J = 7.8 Hz, 1H), 7.28 (d, J = 7.6 Hz, 1H), 7.21 (t, J = 7.1 Hz, 1H), 7.10 (t, J = 7.4 Hz, 1H), 6.70 (s, 1H), 6.28 (s, 1H), 5.35 (d, J = 5.7 Hz, 1H), 4.15 (t, J = 8.6 Hz, 1H), 4.01 (s, 3H), 3.84–3.76 (m, 1H), 3.77 (s, 3H), 3.26 (dd, J = 8.6, 5.7 Hz, 1H), 2.70 (dd, J = 13.2, 5.3 Hz, 1H), 2.03–1.92 (m, 1H), 0.94 ppm (s, 9H); ^{13}C NMR (75 MHz, $CDCl_3$): δ = 204.4 (CO), 148.3 (C), 147.7 (C), 139.0 (C), 135.6 (C), 131.5 (CH), 127.0 (C), 121.4 (CH), 120.3 (CH), 119.4 (CH), 112.1 (C), 108.9 (CH), 100.1 (CH), 78.9 (OCH), 67.0 (OCH_2), 57.8 (OCH_3), 52.1 (C), 46.3 (NCH_3), 34.5 (C), 30.8 (CH), 28.9 (3×CH_3), 26.1 ppm (CH_2); HRMS (EI): m/z calcd for $C_{24}H_{27}O_3N$: 377.1985; found: 377.1984.

6-Butyl-1,2,3a,12c-tetrahydro-4-methoxy-6*H*-benzo[*b*]furo[3″,2″:7′,8′]-cycloocta[3,4]cyclobuta[*b*]furan-7-one (21a): Mixture of diastereoisomers. Yield: 37%; yellow oil; spectroscopic data for the major diastereoisomer; ^{1}H NMR (300 MHz, $CDCl_3$): δ = 8.27 (d, J = 8.2 Hz, 1H), 7.43 (d, J = 8.2 Hz, 1H), 7.37–7.22 (m, 2H), 5.29 (d, J = 3.4 Hz, 1H), 4.47 (d, J = 8.9 Hz, 1H), 4.17–4.12 (m, 1H), 4.05–4.03 (m, 1H), 3.74–3.65 (m, 1H), 3.53 (s, 3H), 2.42–2.30 (m, 2H), 2.11–1.99 (m, 3H), 1.30–1.13 (m, 4H), 0.88 ppm (t, J = 6.7 Hz, 3H); ^{13}C NMR (75 MHz, $CDCl_3$): δ = 190.4 (CO), 162.4 (C), 155.2 (C), 148.5 (C), 146.4 (C), 137.9 (C), 128.9 (C), 126.8 (CH), 126.5 (C), 124.3 (CH), 123.0 (CH), 111.0 (CH), 106.3 (CH), 77.8 (OCH), 66.7 (OCH_2), 57.1 (OCH_3), 51.6 (CH), 45.6 (CH), 29.6 (CH_2), 27.1 (CH_2), 26.4 (CH_2), 25.9 (CH_2), 14.0 ppm (CH_3); HRMS (EI): m/z calcd for $C_{23}H_{24}O_4$: 364.1674; found: 364.1678.

Computational details: All calculations were performed with the Gaussian 03 package of programs.[32] Full geometry optimizations were carried out by using the B3LYP density functional method.[33] This hybrid functional is generally considered a reliable method for transition-metal-containing large molecules.[34] The relativistic effective core potential LANL2DZ[35] for chromium and the standard 6-31G* basis set for hydrogen, carbon, oxygen and nitrogen atoms were employed in the calculations. Harmonic force constants were computed for the optimized geometries to characterise the stationary points as minima or saddle points. Zero-point vibrational corrections were determined from the harmonic vibrational frequencies to convert the total energies E_e to ground-state energies E_0. Intrinsic reaction coordinate calculations were conducted to verify the connection between the transition states and the minimum by

employing the Gonzalez and Schlegel method[36] implemented in Gaussian 03.

ΔG_{gas} values were calculated within the ideal gas, rigid rotor and harmonic oscillator approximations. A pressure of 1 atm and a temperature of 298.15 K were assumed in the calculations. To take into account condensed-phase effects a self-consistent reaction field model (SCRF) was applied. To evaluate the Gibbs solvation energies, single-point energy calculations were performed on the gas-phase structures within the polarizable continuum model (PCM)[37] using the united-atom Hartree–Fock (UAHF) parametrization.[38] ΔG_{soln} was obtained by addition of the solvation Gibbs energy to ΔG_{gas}. A relative permittivity of 7.58 was employed to simulate THF as the solvent used in the experimental work. Unless otherwise indicated, the relative energy values indicated in the discussion will refer to Gibbs energies including the solvation contribution. Computational data, three-dimensional models and cartesian coordinates for all the stationary points found are included in the Supporting Information.

Acknowledgements

We thank the Dirección General de Investigación (DGI) of Spain for financial support of this work. A FPU predoctoral fellowship from the Ministerio de Educación y Ciencia of Spain to M.F.-M. is gratefully acknowledged.

[1] Part of this work has previously been published as a communication: J. Barluenga, F. Aznar, M. A. Palomero, *Angew. Chem.* **2000**, *112*, 4514–4516; *Angew. Chem. Int. Ed.* **2000**, *39*, 4346–4348.

[2] K. H. Dötz, *Metal Carbenes in Organic Synthesis*, Springer, New York, **2004**.

[3] For general reviews, see: a) W. D. Wulff in *Comprehensive Organometallic Chemistry II, Vol. 12* (Eds.: E. W. Abel, F. G. A. Stone, G. Wilkinson), Pergamon Press, New York, **1995**, p. 469; b) K. H. Dötz, P. Tomuschat, *Chem. Soc. Rev.* **1999**, *28*, 187.

[4] a) W. D. Wulff, G. A. Peterson, P. C. Tang, R. W. Kaesler, *J. Am. Chem. Soc* **1985**, *107*, 1060–1062; b) B. A. Anderson, J. M. Bao, T. A. Brandvold, C. A. Challener, W. D. Wulff, Y. C. Xu, A. L. Rheingold, *J. Am. Chem. Soc.* **1993**, *115*, 10671–10687.

[5] a) K. H. Dötz, R. E. Dietz, *J. Organomet. Chem.* **1978**, *157*, C55; b) E. Chelain, R. Goumont, L. Hamon, A. Parlier, M. Rudler, H. Rudler, J. C. Daran, J. Vaissermann, *J. Am. Chem. Soc.* **1992**, *114*, 8088–8098; c) T. Ishibashi, N. Ochifuji, M. Mori, *Tetrahedron Lett.* **1996**, *37*, 6165–6168.

[6] D. F. Harvey, D. M. Sigano, *Chem. Rev.* **1996**, *96*, 271–288.

[7] a) A. Yamashita, *Tetrahedron Lett.* **1986**, *27*, 5915–5918; b) A. de Meijere, *Pure. Appl. Chem.* **1996**, *68*, 61–72; c) R. Aumann, H. Heinen, M. Krebs, *Chem. Ber.* **1991**, *124*, 2343–2347.

[8] C. A. Challener, W. D. Wulff, B. A. Anderson, S. Chamberlain, K. L. Faron, O. K. Kim, C. K. Murray, Y. C. Xu, D. C. Yang, S. D. Darling, *J. Am. Chem. Soc.* **1993**, *115*, 1359–1376.

[9] a) F. Hoffmann, S. Siemoneit, M. Nieger, K. Sirpa, K. H. Dötz, *Chem. Eur. J.* **1997**, *3*, 853–859; b) K. H. Dötz, S. Siemoneit, F. Hoffmann, M. Nieger, *J. Organomet. Chem.* **1997**, *541*, 285–290.

[10] K. H. Dötz, *Angew. Chem.* **1975**, *87*, 672–673; *Angew. Chem. Int. Ed. Engl.* **1975**, *14*, 644–645.

[11] A. de Meijere, H. Schirmer, M. Duetsch, *Angew. Chem.* **2000**, *112*, 4124–4162; *Angew. Chem. Int. Ed.* **2000**, *39*, 3964–4002.

[12] Loss of CO ligand: a) H. Fischer, K. H. Dötz, R. Markl, J. Muhlemeier, *Chem. Ber.* **1982**, *115*, 1355–1362; b) M. M. Gleichmann, K. H. Dötz, B. A. Hess, *J. Am. Chem. Soc.* **1996**, *118*, 10551–10560; c) J. Barluenga, F. Aznar, A. Martín, S. García-Granda, E. Pérez-Carreño, *J. Am. Chem. Soc.* **1994**, *116*, 11191–11192; d) J. Barluenga, F. Aznar, I. Gutiérrez, A. Martín, S. García-Granda, M. A. Llorca-Baragaño, *J. Am. Chem. Soc.* **2000**, *122*, 1314–1324; e) H. Fischer, P. Hofmann, *Organometallics* **1999**, *18*, 2590–2592.

[13] Acetylene coordination: a) K. H. Dötz, T. Schäfer, F. Kroll, K. Harms, *Angew. Chem.* **1992**, *104*, 1257–1259; *Angew. Chem. Int. Ed. Engl.* **1992**, *31*, 1236–1238; b) K. H. Dötz, S. Siemoneit, F. Hohmann, M. Nieger, *J. Organomet. Chem.* **1997**, *541*, 285–290.

[14] Alkyne insertion: a) P. Hofmann, M. Hämmerle, *Angew. Chem.* **1989**, *101*, 940–942; *Angew. Chem. Int. Ed. Engl.* **1989**, *28*, 908–910; b) P. Hofmann, M. Hämmerle, G. Unfried, *New J. Chem.* **1991**, *15*, 769–789; c) K. E. Garrett, J. B. Sheridan, D. B. Pourreau, W. C. Feng, G. L. Geoffroy, D. L. Staley, A. L. Rheingold, *J. Am. Chem. Soc.* **1989**, *111*, 8383–8391.

[15] CO insertion: a) K. H. Dötz, *Angew. Chem.* **1979**, *91*, 1021–1022; *Angew. Chem. Int. Ed. Engl.* **1979**, *18*, 954–955; b) B. A. Anderson, W. D. Wulff, A. L. Rheingold, *J. Am. Chem. Soc.* **1990**, *112*, 8615–8617; c) A. Mayr, M. F. Asaro, T. J. Glines, *J. Am. Chem. Soc.* **1987**, *109*, 2215–2216.

[16] Electrocyclic ring closure: a) P. C. Tang, W. D. Wulff, *J. Am. Chem. Soc.* **1984**, *106*, 1132–1133; b) W. D. Wulff, B. M. Bax, T. A. Brandvold, K. S. Chan, A. M. Gilbert, R. P. Hsung, J. Mitchell, J. Clardy, *Organometallics* **1994**, *13*, 102–126; c) M. Torrent, M. Duran, M. Solà, *Chem. Commun.* **1998**, 999–1000; d) M. Torrent, M. Duran, M. Solà, *J. Am. Chem. Soc.* **1999**, *121*, 1309–1316.

[17] a) K. H. Dötz, R. Dietz, *Chem. Ber.* **1978**, *111*, 2517–2526; b) A. Yamashita, T. A. Scahill, C. G. Chidester, *Tetrahedron Lett.* **1985**, *26*, 1159–1162; c) K. S. Chan, W. D. Wulff, *J. Am. Chem. Soc.* **1986**, *108*, 5229–5236; d) W. E. Bauta, S. F. Pavkovic, W. D. Wulff, E. J. Zaluzec, *J. Org. Chem.* **1989**, *54*, 3249–3252; e) J. F. Quinn, M. E. Bos, W. D. Wulff, *Org. Lett.* **1999**, *1*, 161–164.

[18] For some representative examples, see: a) K. H. Dötz, W. Khun, *Angew. Chem.* **1983**, *95*, 750–751; *Angew. Chem. Int. Ed. Engl.* **1983**, *22*, 732; b) W. D. Wulff, Y. C. Xu, *J. Am. Chem. Soc.* **1988**, *110*, 2312–2314; c) D. L. Boger, O. Huter, K. Mbiya, M. S. Zhang, *J. Am. Chem. Soc.* **1995**, *117*, 11839–11849; d) A. Minatti, K. H. Dötz, *J. Org. Chem.* **2005**, *70*, 3745–3748.

[19] a) J. Barluenga, F. Aznar, M. A. Palomero, S. Barluenga, *Org. Lett.* **1999**, *1*, 541–543; b) J. Barluenga, M. A. Fernández-Rodríguez, F. Andina, E. Aguilar, *J. Am. Chem. Soc.* **2002**, *124*, 10978–10979.

[20] For a similar tandem cycloaddition–alkyne-insertion–cyclization process of Fischer carbene complexes, see: S. Chamberlain, W. D. Wulff, B. Bax, *Tetrahedron* **1993**, *49*, 5531.

[21] a) J. E. Saxton, *The Chemistry of Heterocyclic Compounds*, Wiley, Chichester, **1994**, Vol. 25, Part IV; b) J. E. Saxton, *Nat. Prod. Rep.*.**1997**, *14*, 559–590; c) J. E. Saxton in *The Alkaloids* (Ed.: G. A. Cordell), Academic Press, New York, **1998**, Vol. 50, Chapter 9; d) J. E. Saxton in *The Alkaloids* (Ed.: G. A. Cordell), Academic Press, New York, **1998**, Vol. 51, Chapter 1; e) M. Toyota, M. Ihara, *Nat. Prod. Rep.*.**1998**, *15*, 327–340; f) K. C. Nikolau, S. A. Snyder, *Classics in Total Synthesis II*, Wiley-VCH, Weinheim, **2003**, Chapters 5, 8, 12, 18–20 and 22, p. 639.

[22] K. Miwa, T. Aoyama, T. Shioiri, *Synlett* **1994**, 107–108.

[23] For electrocyclization reactions involving the 2,3-indole bond, see: a) H. Hawagira, T. Choshi, H. Fijimoto, E. Sugino, S. Hibino, *Tetrahedron* **2000**, *56*, 5807–5811; b) S. Tohyama, T. Choshi, K. Matsumoto, A. Yamabuki, K. Ikegata, J. Nobuhiro, S. Hibino, *Tetrahedron Lett.* **2005**, *46*, 5263–5264.

[24] a) B. C. Maiti, R. H. Thomson, M. Mahendran, *J. Chem. Res. (S)* **1978**, 126–127; b) R. J. Capon, E. L. Ghisalberti, P. R. Jefferies, *Phytochemistry* **1983**, *22*, 1465–1467.

[25] J. R. Knox, J. Slobbe, *Aust. J. Chem.* **1975**, *28*, 1843–1856.

[26] a) M. M. Gleichmann, K. H. Dötz, B. A. Hess, *J. Am. Chem. Soc.* **1996**, *118*, 10551–10560.

[27] Most of the attempts to find a transition state for the carbonyl insertion from **A1** ended up with a different saddle point that corresponds to the transition state for the formation of a C–C bond between C1 and C7, and which leads to the formation of a seven-membered carbocycle. This saddle point has an energy 3.2 kcal mol^{-1} greater than **TS(A3→A8)**.

[28] Z. Otwinowski, W. Minor, *Methods Enzymol.* **1997**, *276*, 307–326.

[29] R. H. Blessing, *Acta Crystallogr. Sect. A* **1995**, *51*, 33–38.

[30] A. Altomare, G. Cascarano, C. Giacovazzo, A. Guagliardi, M. C. Burla, G. Polidori, M. Camalli, *J. Appl. Crystallogr.* **1994**, *27*, 435–436.
[31] SHELXL-97, Program for the Refinement of Crystal Structures, G. M. Sheldrick, University of Göttingen, Göttingen, Germany, **1997**.
[32] Gaussian 03, Revision C.02, M. J. Frisch, G. W. Trucks, H. B. Schlegel, G. E. Scuseria, M. A. Robb, J. R. Cheeseman, J. A. Montgomery, Jr., T. Vreven, K. N. Kudin, J. C. Burant, J. M. Millam, S. S. Iyengar, J. Tomasi, V. Barone, B. Mennucci, M. Cossi, G. Scalmani, N. Rega, G. A. Petersson, H. Nakatsuji, M. Hada, M. Ehara, K. Toyota, R. Fukuda, J. Hasegawa, M. Ishida, T. Nakajima, Y. Honda, O. Kitao, H. Nakai, M. Klene, X. Li, J. E. Knox, H. P. Hratchian, J. B. Cross, C. Adamo, J. Jaramillo, R. Gomperts, R. E. Stratmann, O. Yazyev, A. J. Austin, R. Cammi, C. Pomelli, J. W. Ochterski, P. Y. Ayala, K. Morokuma, G. A. Voth, P. Salvador, J. J. Dannenberg, V. G. Zakrzewski, S. Dapprich, A. D. Daniels, M. C. Strain, O. Farkas, D. K. Malick, A. D. Rabuck, K. Raghavachari, J. B. Foresman, J. V. Ortiz, Q. Cui, A. G. Baboul, S. Clifford, J. Cioslowski, B. B. Stefanov, G. Liu, A. Liashenko, P. Piskorz, I. Komaromi, R. L. Martin, D. J. Fox, T. Keith, M. A. Al-Laham, C. Y. Peng, A. Nanayakkara, M. Challacombe, P. M. W. Gill, B. Johnson, W. Chen, M. W. Wong, C. Gonzalez, J. A. Pople, Gaussian, Inc., Pittsburgh, PA, **2003**.
[33] a) A. D. Becke, *J. Chem. Phys.* **1993**, *98*, 5648–5652; b) A. D. Becke, *Phys. Rev. A* **1988**, *38*, 3098–3100; c) C. Lee, W. Yang, R. G. Parr, *Phys. Rev. B* **1988**, *37*, 785–789.
[34] For some recent computational work on organometallic species, see: a) S. Kozuch, C. Amatore, A. Jutand, S. Shaik, *Organometallics* **2005**, *24*, 2319–2330; b) T. Sordo, P. Campomanes, A. Diéguez, F. Rodríguez, F. J. Fañanás, *J. Am. Chem. Soc.* **2005**, *127*, 944–952; c) J. J. Lippstreu, B. F. Straub, *J. Am. Chem. Soc.* **2005**, *127*, 7444–7457.
[35] P. J. Hay, W. R. Wadt, *J. Chem. Phys.* **1985**, *82*, 270–283.
[36] a) C. Gonzalez, H. B. Schlegel, *J. Chem. Phys.* **1989**, *90*, 2154–2161; b) C. Gonzalez, H. B. Schlegel, *J. Phys. Chem.* **1990**, *94*, 5523–5527.
[37] a) J. Tomasi, M. Persico, *Chem. Rev.* **1994**, *94*, 2027–2094; b) J. Tomasi, R. Cammi, *J. Comput. Chem.* **1995**, *16*, 1449–1458.
[38] V. Barone, M. Cossi, J. Tomasi, *J. Chem. Phys.* **1997**, *107*, 3210–3221.

Received: March 14, 2007
Revised: May 3, 2007
Published online: July 2, 2007

